The International Journal of Medical Robotics and Computer Assisted Surgery

Patient specific customized cranioplasty by 3D printing of biopolymers, 3D printed molds and silicone molds

Journal:	*The International Journal of Medical Robotics and Computer Assisted Surgery*
Manuscript ID	RCS-22-0228.R1
Wiley - Manuscript type:	Original Article (Direct Via EEO)
Date Submitted by the Author:	19-Jun-2023
Complete List of Authors:	Flora, Barbara; University of Rome Tor Vergata, Department of Clinical Sciences and Medicine; University of Rome Tor Vergata, CIMER, Interdepartmental Centre for Regenerative Medicine Scerrati, alba; University of Ferrara, Department of Translational Medicine, University of Ferrara, Ferrara, Italy Trovalusci, Federica; University of Rome Tor Vergata, Enterprise Engineering vesco, silvia; University of Rome Tor Vergata, Enterprise Engineering
Primary Area:	Technical
Anatomy Keywords:	craniofacial, bone
Operation Keywords:	osteotomy
Specialty Keywords:	reconstruction, maxillofacial
Technology Keywords:	additive manufacturing, prosthetics
Keywords:	patient-customized prosthesis, implantable FDM filament, medical-grade materials
Abstract:	With the advancement of 3D printing technologies, the possibility of manufacturing patient-specific cranioplasty has emerged as an alternative to autologous bone. In this study, three different strategies using fused deposition modelling (FDM) additive manufacturing (AM) were applied and compared: (i) direct printing of PLA (polylactic acid) prosthesis, mould casting of poly(methyl methacrylate) (PMMA) prosthesis using (ii) silicone mould, (iii) thermoplastic poly urethane (TPU). All techniques studied achieved good geometric accuracy and cosmetic appearance. Direct printing of the PLA prosthesis resulted in the fastest strategy, followed by PMMA casting in silicone mould. Nevertheless, the use of silicone mould led to many advantages, such as lower costs and the possibility of using autoclaving as a sterilisation technique.

Reviewer 1

Minor:

An extensive editing work has been done on the paper. In order to avoid a heavy cluttering of the text, these changes are not evidenced.

Major:

- Introduction has been deeply reviewed and summarized, please find changes reported in red. Also, strategies and purposes of the study has been clarified.
- Extra details on the procedures (details on software, hardware, material, factories, brand etc..) has been added to the text, in particular in sections 2.1, 2.2.2, 2.2.3. Please find modifications in red. Considerations on sterilization processes were also included (
- Financial analysis has been conducted again, in particular including depreciation of machines, cost-per-hour of personnel units, materials, and measuring effectively energy consumption. Please find a more detailed discussion in section 3.2, 3.3, 3.4.
- Discussion of the results has been completely reviewed in a more straight and clear form. Please find modifications in section 4.

Reviewer 2

- The optimization of the manufacturing strategies was done upstream, acting only on the most process-dependent step: additive manufacturing. Since printing conditions were critical in terms of printing time, we prioritized this last aspect rather than mechanical properties which, from previous experience, still resulted in the range of efficiency good for our purposes for the printing conditions adopted.
- Nevertheless, a mechanical characterization was conducted to compare the three different implementation strategies, and the orientation of the filament with respect to the growing direction of the model. Samples were then also characterized in terms of roughness. Please find these integration, in particular in sections 2.3 and 3.5
- Study of biocompatibility was out of the goals and the competences of this study since it would require a study on its own.

Reviewer 3

- To amend the differences between the procedure adopted in the calculation of current costs of the three strategies, these where calculated again adopting the same routine. The so-obtained cost was also compared to the commercial one for silicone-mold scenario. Please find modifications in 3.2, 3.3, 3.4.

Patient specific customized cranioplasty by 3D printing of biopolymers, 3D printed molds and silicone molds.

Flora B[1-2], Scerrati A[3,4], Trovalusci F[5], Vesco S[5]

[1]Department of Clinical Sciences and Medicine, University of Rome "Tor Vergata", Rome, Italy
[2]CIMER, Interdepartmental Centre for Regenerative Medicine, University of Rome "Tor Vergata", Rome, Italy
[3]Neurosurgery, Sant'Anna University Hospital Ferrara, Ferrara, Italy;
[4]Department of Translational Medicine, University of Ferrara, Ferrara, Italy;
[5]Department of Enterprise Engineering, University of Rome "Tor Vergata", Rome, Italy.

Abbreviations

ABS: Acrylonitrile Butadiene Styrene
AM: Additive Manufacturing
BVOH: Butenediol Vinyl Alcohol Copolymer
CT: Computed Tomography
FDM: Fused Deposition Modelling
HPGP: Hydrogen Peroxide Gas Plasma
PEEK: (poly ether ether ketone)
PLA: Poly Lactic Acid
PMMA: Poly(methyl methacrylate)
TPU: Thermoplastic Polyurethane

Keywords: Bone, craniofacial, reconstruction, additive manufacturing, prosthetics, patient-customized prosthesis, implantable FDM filament, medical-grade materials.

Abstract

With the advancement of 3D printing technologies, the possibility of manufacturing patient-specific cranioplasty has emerged as an alternative to autologous bone.

In this study, three different strategies using fused deposition modelling (FDM) additive manufacturing (AM) were applied and compared: (i) direct printing of PLA (polylactic acid) prosthesis, mold casting of poly(methyl methacrylate) (PMMA) prosthesis using (ii) silicone mold, (iii) thermoplastic poly urethane (TPU).

All techniques studied achieved good geometric accuracy and cosmetic appearance.

Direct printing of the PLA prosthesis resulted in the fastest strategy, followed by PMMA casting in silicone mold. Nevertheless, the use of silicone mold led to many advantages, such as lower costs and the possibility of using autoclaving as a sterilization technique.

1. Introduction

In the craniofacial region, trauma and tumors are common pathologies that may require the restoration of a small or large amount of osteocartilaginous tissue. In cranioplasty procedure, the replacement of the missing bone has a positive influence on both physical and neurological state of the patient, leading to reduction of healing time, preservation of the underlying brain and improvement of the patient's appearance (1) (2).

This clinical procedure usually involves the use of prostheses made of various materials, allogenic or not, such as titanium (Ti), ceramic, polymeric or transplanted bone materials (3) (4). In some cases, the primary tissue for cranioplasty is autologous bone (5) (6). However, this strategy is limited by the potential for bone resorption.

Titanium has anti-inflammatory and non-corrosive properties, but may cause an increase in hypersensitivity due to prolonged and continuous exposure to this metal (7). The most popular implantable polymers are PEEK (polyetheretherketone) and PMMA (8) (9).

In particular, PEEK shows excellent implant success due to its high biocompatibility, although the risk of prosthesis rejection is not completely eliminated (10). It has excellent mechanical resistance and is easy to machine (11). However, PEEK polymer is not the standard choice for cranioplasty due to the high cost of material and processing equipment (12). In addition, the lack of radiopacity of PEEK may interfere with the radiologic imaging technique used to evaluate prosthesis placement (13).

PMMA is the most widely used polymeric material for cranioplasty, offering the best compromise between mechanical properties, biocompatibility and cost. PMMA exhibits high mechanical resistance at compression, good heat resistance (3), and leads to a higher rate of infection (10).

Both PEEK and PMMA are suitable for 3D printing. (14). This customizable manufacturing process has emerged in recent years in medicine for its potential in creating patient-specific prostheses.

A missing part of a bone is replicated by processing a high-resolution computed tomography (CT) scan of the head with appropriate CAD software (15). The use of a native model greatly improves the quality of the prosthetic design (16).

The prosthetic system can be prefabricated or fabricated during the preoperative phase using 3D printers (17), reproducing the patient's specific skull geometry previously determined by CT (18). However, the cost of industrial and commercial 3D printers has kept 3D printing from being widely adopted.

In recent years, the introduction of desktop 3D printers has lowered the cost of these machines (17); on the other hand, 3D printing of custom molds (mono- or bi-valves) has emerged as an alternative process to direct 3D printing of a cranial flap with thermoplastic filament (19).

This alternative strategy allows the use of non-printable polymeric materials, such as liquid medical grade PMMA oligomer. The technique consists of directly printing a mold using a thermoplastic filament, such as PLA. The thermoplastic material can be chemically inert and medical grade to create a mold that can be used in direct contact with the liquid oligomer used for casting (e.g. PMMA) (18). Alternatively, a low-cost non-medical material can be used for printing by covering the mold with special sterile plastic bags (e.g., surgical incision drape (17), silicone layer (19)). However, special attention must be paid to the choice of the cover material, since the exothermic phase of polymerization of the cast oligomer may affect the surface of the bag, leading to partial dissolution and release of chemicals (20).

Another aspect to consider in the casting strategy is the assessment of skin contracture prior to implant design (21). Finally, the cast mold models may require post-processing adjustments related to the coupling of bi-valve molds (17) (20).

The present study will provide a comparison between three main strategies for AM fabrication of cranial prostheses: direct 3D printing of prostheses, use of a 3D printed rigid mold, and use of a soft mold obtained from a 3D printed bone master.

2. Materials and methods

2.1 DICOM files processing

The three techniques presented here for the realization of a patient-specific prosthesis all share a common procedure for the elaboration of the model, which represents the first step of the methods. This is the acquisition of the anatomy of the patient's skull, prior to the decompressive craniotomy, by CT and its storage as DICOM files. The DICOM files are processed by using, in sequence, the software InVesalius 3.1, VxElements, Meshmixer, Simplify3D.

InVesalius, version 3.1, (Invesalius, Brazil) is an open source software used to translate DICOM files into 3D image files. The software is programmed for the reconstruction of computed tomography and

magnetic resonance images and their advanced 3D visualization. The software is equipped with image segmentation and measurement tools.

VxElements (Ametek Creaform, Italy) is an open source, post-processing, scan-to-CAD software module to be integrated with the use and design of CAD software. Vx Element is designed for the optimization of the mesh: here has been used to remove fictive structure errors.

The output files, consisting of 3D images of a surface, are then processed by Meshmixer 3.5 software to perform thickening. Meshmixer is a state-of-the-art, open-source software for working with triangular meshes, published by Autodesk Ireland Corporation UC, Ireland. The prosthesis models were then thickened with different values depending on the final implementation technology. Direct printing of the prosthesis required a model thickness of 3.00 mm (i.e., the average dimension of the original cranial bone). The same model was used to project the TPU mold. The master model used to shape the silicone mold was designed with a thickness of 5.00 mm. The larger space in the lumen of the mold was provided taking into account the space required for the allocation of the upper valve of the mold (lid).

A second meshing using Meshmixer completes the process to reduce the degree of error that may occur during thickening operations.

Prior to direct printing of the PLA cranial flap, the file from Meshmixer is processed using Z-Suite (Zortrax Software, Zortrax S.A., Poland) to perform slicing, set the orientation of the model, and position the pillars and supports.

In the procedure that includes the production of the silicone mold, the file in the output of Meshmixer is processed by the open source software Simplify3D, version V4 (Simplify 3D; Italy). This is a specific software compatible with the use of Delta printers (see section 2.2.2) and designed for the slicing process and other operations that precede the printing step. In fact, in the same phase, the printing orientation and the positioning of the columns are added to the model using the same software. An orientation with the concavity facing down is set.

In the development of two-valve, TPU mold method, the designs of the two half of the molds, superior and inferior, is carried out processing the model by using SolidWorks software (Dassault Systèmes, France), and Z-Suite in sequence, to return two separate .zcode files. In this case, Z-Suite is also used to perform the slicing process instead of Simplify3D software.

All the STL files have been projected, oriented and optimized for the shortest printing time.

2.2 Cranioplasty implementation

2.2.1 3D direct printing of biopolymers

Direct printing of the cranial portion identified for the implementation of the prosthesis was performed using the STL file described in Section 2.1. A non-implantable medical grade PLA

filament was selected to proceed with the printing feasibility studies. Namely, PLA bone Healthfil (Treed Filaments, Seregno (MB), Italy), was chosen because of its mechanical properties and texture, which accurately reproduce the behavior of natural bone. The printing process was performed using a Zortrax M300 Dual FDM printer. The processing parameters are shown in Table 1.

Table 1: Operative parameters for the printing process of PLA filament

2.2.2 PMMA casting by silicone molds

Silicone molds were realized by a specific company of 3D printing (CAD Ortopedia, S.r.l., U.s., Ganzanigo, BO). The mold was made using as a master an ABS (Acrylonitrile Butadiene Styrene) printed model of the missing cranial flap. The master was obtained by 3D printing an ABS filament (Wasp S.r.l., Italy) using a nozzle temperature of 220 °C, a bed temperature of 55 °C, a standard printing speed of 45 mm/s, a x/y axis movement speed of 150 mm/s, and a z axis movement speed of 150 mm/s. The film thickness was set to 0.15 mm.

An industrial printer, Delta Wasp 4070 (Wasp S.r.l, Italy), was used in the process (15). Figure 1 shows the image of the 3D printed master in ABS.

Figure 1 3D-printed master in ABS of the cranial flap.

The silicone mold was composed of 2 complementary pieces. A 1 cm diameter hole was left at the highest point of the mold profile to allow the poured PMMA (Cranioplastic, Codman& Shurtleff, inc., USA) to complete filling of the mold. A schematic illustration of the mold is shown in Figure 2.

Figure 2 Schematic representation of the silicon mold during the phase of cranial flap extraction

2.2.3 PMMA casting by 3D printed TPU molds.

The 3D printing of the two valves was performed using an elastic TPU filament (Elasto A, Treed Filaments, Seregno (MB), Itay). A Zortrax M300 Dual printer (Zortrax S.A., Poland) was used for the additive manufacturing process. The processing parameters defined using the corresponding Z-Suite 2 (version 2.23.0) slicing software (printer software, Zortrax S.A., Poland) and tested in preliminary studies are shown in Table 2.

Table 2 Operative parameters in the printing process of two valves mold using TPU filament

Liquid PMMA (Cranioplastic, Codman& Shurtleff, inc., USA) was then poured into the TPU mold through the hole at the top, following the procedure described in 2.2.2.

2.3 Characterization

The mechanical properties of skull tops and their dependence on the printing direction of: the prosthesis ("direct print" strategy), the master ("silicone mold" strategy), or the mold ("TPU mold" strategy), were evaluated by flexure tests.

The test specimens were obtained by controlling the printing direction, which is considered to be the direction of growth of the deposited layers. Two main axes were considered: "parallel" axis (or direction) consists in the axis that runs parallel to the plane where a deposited filament lies, "orthogonal axis" runs parallel to the growth direction of the layers.

Rectangular samples were obtained in the two directions, with dimensions of (127.00 x 12.70 x 3.00) mm, according to ASTM D790 standard, for each of the three fabrication approaches.

Specimens obtained by direct 3D printing of PLA were implemented so that their growth direction was parallel or perpendicular to the longest edge of the disc (Figure 3). STL file of the samples is shown in (Figure 3-a and Figure 3-b). The blue arrow indicates the growth direction of the layers. Printing conditions and materials are the same as described in section 2.2.1.

Figure 3 "Direct print"scenario: STL files file of a) parallel and b) orthogonal samples; c) printed samples in the two orientations

Rectangular specimens, representative of the scenario of PMMA casting through silicone molds, were prepared following an operational procedure analogous to that described in section 2.2.2. ABS masters of the rectangular specimens required for the silicone mold were printed using the same orientation adopted for the PLA disks (same STL file reported in Figure 3). The printing conditions were the same as for ABS reported in 2.2.2. ABS discs were immersed in a silicone pot. After the silicone was cured (Figure 4-a), the ABS specimens were manually removed. Sockets formed by ABS discs were then filled with liquid PMMA. After curing, PMMA disks characterized by two orientations, orthogonal and parallel, were removed (Figure 4-b).

Figure 4 "silicone mold" scanario: a) preparation of silicone mold with ABS masters; b) cast samples in the two orientations.

STL files of TPU molds for PMMA casting, along the two directions, are reported in (Figure 5-a, Figure 5-b). The growth direction of TPU filament deposition is indicated by the blue arrow reported in the figure, where mold cavities are also visible. Nevertheless, the mold cavities were implemented with rectangular geometry of (127.00 x 12.70 x 3.00) mm dimension.

Figure 5 "TPU mold" scenario: STL file of a) parallel mold and b) orthogonal mold; c) cast samples in the two orientations

Slices obtained after PMMA casting and curing are shown in Figure 5-c.

Bending property tests were performed on the above disks in accordance with ASTM D790.

The finish of the samples was analyzed using an inductive profilometer (TalySurf CLI 2000, Taylor Hobson, Leicester, UK) to evaluate the influence of the manufacturing strategies on the texture of the outer surface. An area of 4x4 mm2 was scanned with a resolution of 1 mm to evaluate the roughness parameters and to construct the corresponding 3D maps. Data processing was performed using TalyMap 3.1 software (Taylor Hobson, Leicester, UK).

Dimensional accuracy was determined on each dimension (thickness, width, length) using Equation 1:

Eq. 1 $\Delta\ \% = \frac{(D_p - D_a)}{D_p}\ 100$

Where:

$D_p =$ Dimension provided by the project (thickness/width/length)

$D_a =$ Average dimension (thickness/width/length)

Dimensions were determined by caliper measurement (Z22855F, OWIM GmbH & Co., Germany).

The energy consumption associated with the manufacturing process was evaluated by measuring the electrical energy consumed during the printing process using a plug-in power meter socket (model PM01, Maxcio, China).

3. Results

3.1 DICOM files processing

High-resolution CT scans of the preoperative patient's skull were performed and processed to obtain the STL file for reconstruction of the defected area after surgery. In this way, the elaboration of the DICOM file did not require any processing of virtual reconstruction of the missing bone (mirroring of the whole skull section, opposite to the removed section, interpolation or graphical restoration).

The results of DICOM file processing are shown in Figure 6. In particular, Figure 6-a shows the output image immediately after processing by VxElement, where a 3D image is created and fictive structures are removed, where the spikes or lumps are removed. The latter image, when imported and opened with Meshmixer, appears in Figure 6-b. The image shows an irregular mesh (automatically applied by the software) of a 2D surface with no thickness applied. Some errors created during the file import were removed in the same step, as can be seen in the magnification. The imported file was then processed by Meshmixer to obtain a thickening of 3 mm or 5 mm, depending on the

manufacturing method. After thickening, a second meshing procedure was applied to remove errors from the thickening step (Figure 6-c).

Figure 6: Images of a selected section of patient's cranium, selected as model for the implant manufacturing: a) 3D model of cranium surface; b) same surface after meshing process; c) model after thickening and the second step of meshing.

The images were then ready to be processed to perform the slicing step, set the printing orientation of the skull cap, and design the supports and pillars.
Direct printing of the PLA cap requires the Z-Suite software to perform slicing as it is compatible with the Zortrax M300 Dual FDM printer (Figure 7).

Figure 7 Slicing file of 3 mm PLA skull cap.

The design of the TPU mold was performed by processing the Meshmixer output file using SolidWorks software. In this step, the structures of the two valves of the mold were designed (Figure 8-a). As for the PLA cap, the TPU mold design file was sliced and adapted to the printing step using Z-Suite (Figure 8-b).

Figure 8 3D image of a) upper mold half (left) in upside down position, and lower mold half (right) in upside down position; b) slicing files of structures as in a)

The elaboration process, from DICOM to printing the STL file, was shared among the three manufacturing methods. However, the process time for the realization of the 5 mm ABS master was longer due to the higher number of iterations performed in a thicker model. In addition, the TPU bi-valve mold required additional time due to the SolidWorks projection of the mold. Also, mesh refinement and slicing procedures were required to process both files using Z-Suite software.
The slicing and image processing procedures were performed by a specialized computer technician and a radiology technician. The different steps of a standard case in which no noise or anomalies were found, and the personnel involved in each step, are shown in Table 3.

Table 3 Step timing, men hours and software used for the elaboration of each step from DICOM file to printing file

3.2 Biopolymer cranioplasty

An image of the resulting cranial flap is shown in Figure 9. The images show the use of two different materials: one for printing the skull prosthesis (PLA, non-implantable medical grade), the second for

the realization of the raft and the pillars (butenediol vinyl alcohol copolymer (BVOH)_Z-Support Premium, which is compatible with PLA).

This choice was made intentionally to reduce the cost of the materials. In fact, the implantation implies the change from medical grade PLA filament (used in this study) to implantable grade PLA filament. The amount of BVOH consumed for the deposition of the supports was 17.02 g, which represents approximately 43% of the total material consumed in the printing, being the amount of PLA consumed for the cranial flap of 45.02 g. This represents a significant savings since the cost of implantable PLA is reported to be 82.72 per gram (22), while the cost of an 800 g package of support filament was 119.00 € (23). In these quotes, the total price for the materials used in the printing (both PLA and BVOH) was 3724.00 €.

The use of a non-implantable polymer in contact with the implantable prosthesis has been reported in the literature (24) and has been shown not to affect or contaminate the medical quality of the implant when subjected to prior thorough washing (25).

However, the same model can be printed entirely in implantable grade PLA, without significant modification to the printer setup, and still at a reasonable cost (5132.00 €) (23).

Figure 9 Cranial flap obtained from direct printing of PLA filament

The printing time for the realization of the PLA prosthesis takes a total time of 30 h 17 min. This includes the time for segmentation of the DICOM file, the slicing of the STL files, the study and adjustment of the model supports (columns), which takes an average time of 7 h. The average time for printing the results is 22 h 47 min, with an "extra time" of 30 min to be added. The extra time defines the setup of the filaments and the printer, the time for removing the model from the machine and the removal of the supports, all parameters that depend on the operator.

Use of personnel, in accordance with Table 3, including extra time operations, affects the cost of direct printed prosthetic with an intake of 98.49 €. Costs per hour for radiology technician and a PC specialized technician were obtained from talent.com (26).

The total cost of one hour of PC work, including energy consumption and depreciation, was 0.2287 €/h, then 1.60 € for the entire design and cutting of the PLA prosthesis. PC depreciation per hour was calculated on the basis of a two-year lifetime, considering 220 working days per year, a working day of 8 h, with an average initial cost of 800 €. PC energy consumption per hour was measured at 0.013 KWh, with an energy cost of 0.1249 €/KWh, related to PUN value in 2020 (27).

Printing time contributes with a "machine time cost" of 21.9 € for the PLA skullcap. The price includes machine depreciation, from an average initial cost of 4000.00 € (0.91 €/h with 20 hours per

day of unattended working time, for 220 days per year) and energy consumption (0.19 KWh for printing set-up of PLA).

In conclusion, the total cost for the implementation of PLA skullcap was of 5253.99 €.

Table 4 shows the timing of the printing process.

Table 4 Timing in manufacturing process of PLA skull flap by direct printing

3.3 Silicon mold

The silicone molds were made by a specialized external supplier (Cad Ortopedia S.r.l., Ganzanigo (BO), Italy). The total manufacturing time, from master printing to silicone mold forming, was 10 h 50 min. In this way, the process, from conversion of DICOM file to mold achievement takes 23 h and 25 min, while the total manufacturing time, including PMMA coping preparation, resulted of 19 h (Table 5).

Table 5 Timing in manufacturing process of PMMA skull flap by silicone mold

The total cost of the silicone mold was 2700.00 €. This price includes the cost of a single dose of PMMA (330.00 € (28)). Within a certain range (from 1 g to the size of the sterilized package), the cost of PMMA does not really vary, since once the sterilized dose is opened, the excess material must be disposed of. The total cost of the prosthesis was therefore 3030.00 €. The resulting cranial flap is shown in Figure 10.

Figure 10 PMMA cranial flap obtained from silicone mold (15)

For comparison purposes only, the data provided by the company was used to prepare a quotation as if the same method were carried out with the same printer, equipment and personnel as for the other two methods. In this regard, according to Table 3, the cost of personnel was 110.47 €, the cost of equipment was 1.83 € for the PC and 8.5 € for the printer, taking into account depreciation and energy consumption, and the total cost of materials (medical ABS for the model, medical silicone for the mold, implantable PMMA) was 380.61 €. The total cost of the prosthesis was 501.43 €, much lower than the commercial cost.

3.4 TPU mold

Image of two valve mold is reported in Figure 11, Figure 12, and Figure 13.

Figure 11 Views of upper mold half of printed TPU mold.

Figure 12 Views of lower mold half of printed TPU mold.

Figure 13 Views of two valves mold of printed TPU mold.

The timing of each step of the process is shown in Table 6.

Table 6 Timing in manufacturing process of PMMA skull flap by TPU mold

From the values reported in Table 3 and Table 6, the printing phase was the most time-consuming step for this method. It took 1 D 18 h 32 min to print the lower valve of the mold and 2 D 7 h 18 min for the upper part, for a total of 4 D 1 h 50 min. Extra time of 30 min was considered. The total extra time of 1 hour is considered to include the PMMA casting and prosthetic extraction step.

The registered energy consumption per hour in the printing process of TPU was 0.2780 KWh, which is higher than that of PLA or ABS because it requires more energy due to the higher temperature applied. Including the depreciation of the printer of 0.91 € per hour, the total cost of the printing process of the upper and lower mold halves was 92.35 €. Contribution to the cost of PC usage was also higher due to longer elaboration times related to the design and implementation of two molds, with a total expenditure of 4.60 €.

Similarly, personnel costs increased up to $299.95, according to Table 3.

In the post-processing phase, the amount of material used was quantified and this value was used to calculate the cost of this scenario. Specifically: 208.64 g were used to print the upper mold, including raft and supports, while 186.20 g were used to print the lower mold half. Since the cost of the filament was 41.00 € for a 0.5 kg package (i.e. 0.08 €/g), the final cost was 32.38 €. To this cost must be added the price of medical grade PMMA, which contributes to the total cost of 330.00 € (28). Then, the total cost of a prosthesis obtained by TPU casting is of 759.28 €.

3.5 Characterization of skullcaps

Surface roughness and mechanical properties were evaluated to understand the effect of processing technology and processing direction on patient-specific skull caps.

First, the geometric accuracy of the specimens was evaluated.

Table 7 Dimensional accuracy of samples of the three scenarios, obtained in the two main orientations.

Depending on the manufacturing strategy, and processing direction, the sample finishing differs each other, even significantly (Figure 14, Table 8).

Figure 14 Morphological maps under adapted scale (from a) to f) plots) and normalized scale (from a') to f') plots) of slab samples obtaine by: a), a') parallel and b), b') orthogonal PLA direct print; c), c') parallel and d), d') orthogonal silicone mold; e, e') parallel, f), f') orthogonal TPU mold.

Table 8 Arithmetic average height values (Ra) of slabs samples obtained by the three different strategies along the two orientations

Ra values range from the lowest, 2.9 and 2.23 µm, found in the "silicone mold" scenario, to 42 and 37 µm, found in the "TPU mold" scenario. The direct print samples showed Ra values in the middle, with values of 18.7 and 18.22 µm. The influence of the processing direction is reflected in the Ra differences between the corresponding samples. Δ values range from -0.59 µm in "direct print" to a maximum of 5 µm in "TPU mold" scenario. The Ra values in the "direct print" scenario are quite similar in both directions because the surface texture is mostly related to parameters such as filament diameter, infill, spacing, etc. The "silicone mold" scenario also shows a moderate Δ of 0.67 µm, which is also the smoothest sample in this study.

This reflects the mechanical behavior of a soft but fragile material such as silicone, from ribs or notches, contextual to the ABS master removal from the mold, even in a favorable configuration, such as parallel configuration. On the other hand, a combination of elements, such as the high viscosity of uncured PMMA, the local flexibility of silicone and an unfavorable wettability, partially hides the complexity of the printed texture. Nevertheless, the mold thickness is sufficient to ensure the correct shape of the sample.

This reflects the mechanical behavior of a soft but fragile material such as silicone, which loses ribs and notches when the ABS master is removed from the mold, even in a favorable configuration such as parallel. On the other hand, a combination of elements, such as the high viscosity of uncured PMMA, the local flexibility of silicone and an unfavorable wettability, partially hides the complexity of the printed texture. Nevertheless, the mold thickness is sufficient to ensure the correct shape of the sample.

Table 9 Flexural modulus of slabs samples obtained by the three different strategies along the two orientations

Figure 15 Load-displacement curves for flexural tests

In order to compare the influence of filament orientation, a displacement of 3.76 mm was chosen to calculate the differences in load values between the parallel scenarios and the corresponding

orthogonal samples. This value was chosen because it was found to be the average displacement at break achieved by the "direct print - orthogonal" specimen.

The highest mechanical strength was exhibited by samples obtained by direct printing of PLA filament in both directions. "Direct print - orthogonal was found to be the only sample with breakage. A 71.01 N difference in sample response was measured at the set deformation. This scenario resulted in the most network-dependent results, as the filament orientation influences the mechanical properties through most of the sample thickness. In this way, the effect of the parallel oriented filament as a reinforcing rib or the notch occurring between the orthogonally oriented filaments are even more pronounced.

The flexural modulus values of the PMMA specimens produced through the TPU mold are lower than the values registered for the first scenario (direct printing, both orientations). A difference of 22.72 N was found between the two orientations.

Both parallel and orthogonal orientations of the silicone mold scenario showed the lowest flexural modulus. In this scenario, the influence of orientation was negligible because the load is intercalated against the displacement curves. This behavior was probably due to the smoother surface of the specimens (Figure 14), which does not represent a reinforcing rib or notch.

In addition to the influence of the printing direction, the sample material was identified as the most important factor influencing the mechanical properties. This aspect would be even more true (under the same infill and model conditions) when implementing a patient-specific prosthesis, since changes in filament orientation are gradual and intertwined when manufacturing a cupped geometry. The stresses applied to this intricate network partially compensate for each other.

3.6 Sterilization process

The sterilization process is a critical step for the success of implantation surgery. In particular, in addition to removing all colony forming u nits, the process used must not induce degradation or release of toxic substances from the treated surface.

An analysis of the relevant literature identified Hydrogen Peroxide Gas Plasma (HPGP) (29) (30) as a suitable sterilization technique for medical grade PLA, while the use of the traditional autoclave is limited to particularly resistant geometries (for cylindrical shape, a diameter greater than 5 mm) (31). HPGP undergoes a sterilization cycle at 45 °C for 45 min.

Platinum-cured liquid silicone rubber, the specific material widely used in healthcare products due to its stability and inertness, can be safely sterilized in many different ways: autoclave, dry heat or gamma irradiation. In this specific case study, an autoclave cycle of 1 hour at 134°C and 2.7 bar was applied.

Sterilization of TPU filaments has been tested in the literature and has been shown not to alter the biocompatibility of the material in terms of cytotoxicity, nor the mechanical and geometric properties of the phantom (32). This was done using the gamma radiation sterilization method. An irradiation of 40 KGy, according to ISO 11137-2. This irradiation is achievable through a variable time, depending on the minimum intensity of the radiation and processing conditions. The process, usually applied in continuous, can last from hours to days.

4. Discussion

The comparisons between the three methods under analysis are discussed below.

The first aspect considered is the cost of production of the skullcaps.

Direct printing of a PLA skullcap would cost 5254 €. The high cost is mainly due to the implantable PLA filament. The costs of the "silicone mold" and "TPU mold" scenarios were significantly lower, with a current cost of 501 € and 759 €, respectively.

In terms of mechanical resistance, all orientations of the "direct print" and "TPU mold" scenarios showed values of flexural modulus close to, or higher, than both the orientations of the "silicone mold" scenario. Nevertheless, this latter scenario was considered as a reference because the specimens were obtained by a technology already successfully used in clinical practice. The use of direct printing of PLA improved the hardness and flexural stiffness of samples, reaching values up to (2974 ± 5) MPa for parallel orientation, while "silicone mold" - orthogonal samples collapsed in a range of applied stresses from around 5 to over 8 MPa. In these terms, the mechanical behavior of PMMA-containing scenarios, even if characterized by lower rigidity, can be considered "more resilient" for the application selected, since no specific orientation induces fragile behavior.

Implementation time was analyzed considering all steps from the slicing of the DICOM file to the post-processing of the printed skull cap. The processing time was approximately in the same order of magnitude as reported for PLA “direct print” technology and “silicone mold technology”, being 30 h 17' and 19 h 5', respectively. This time was recorded despite the inclusion of some additional steps, namely the manufacturing step of the silicone mold, and PMMA casting and drying. This finding was due to the combination of two elements: the ease of printing ABS compared to PLA filament, and the use of a more expensive/sophisticated printer in the silicone mold scenario. Technology using TPU printed molds, took significantly longer time, 119 h 45', due to the presence of two mold halves to be printed and elaborated.

Since sterilization step is considered, the possibility of using autoclave on silicone mold makes this technology of choice. In fact, autoclave is the most economical strategy, both in terms of initial investment and running costs, compared to gamma irradiation or the HPGP method. Autoclave sterilization and HPGP also have a comparable treatment time (1 hour vs. 45 minutes, respectively).

On the other hand, gamma irradiation, the only strategy currently tested and found to be inappropriate for the sterilization of TPU filament, resulted in (32). This technique, although very effective also in the weft of the printed piece, has several drawbacks, including long treatment times (from hours to days), management of radioactivity and, consequently, high costs.

Direct printing of PLA prostheses has a good potential for standardization in terms of minimizing operator-dependent variability. The printing phase provides a part with a fairly reliable profile compared to the original model.

A second method for the realization of a cranial prosthesis considers the production of a silicone mold. The design of the printing model does not really require any modification, since silicone molds are made by hand on a master printed in ABS, following a procedure that is completely analogous to the direct printing of the PLA prosthesis. The preparation of the silicone mold is done manually, therefore it takes some time and its quality depends on the operator.

The "TPU mold" strategy differs from the previous two since the CT image processing and file elaboration involves the design of a separate file for each of the two valves of the mold. This step requires the intervention of an operator whose ability depends on the efficiency of the mold, the amount of TPU filament consumed and the printing time. Nevertheless, for this method, the intervention of operator in the manufacturing of molds is not required as for the silicone mold, specifically in the mold manufacturing step. This provides the "TPU mold" method with a higher potential of automation, as the main advantage over the use of silicone mold.

PMMA implants have a biocompatibility and induce an inflammatory that are more compatible, compared to PLA, with the implementation of large-size implants. Nevertheless, the implantation of PMMA prosthesis require to ensure the complete polymerization of PMMA to avoid the exposure of neural tissue to the heat generated during polymerization (21), or the contact with unreacted chemicals. In this scenario, casting is the critical step. The mold could be realized in silicone or in TPU, and these materials are both good choices (33). Although the release of traces of TPU during polymerization of PMMA needs to be evaluated in future studies, a review of the relevant literature suggests that TPU is a material with a reduced induction of inflammatory response (34).

Conclusions

Three procedures were discussed here for the implementation of cranioplasty. Among these three, the "silicone mold" scenario presented the highest number of beneficial, according to most of the evaluation criteria considered. In particular, the possibility of using implantable PMMA for the manufacture of the skullcap, a material that features a lower inflammatory response, as a higher compatibility, with respect to PLA. Implantable PMMA is supplied as a sterile product, so the only

part that needs to be sterilized is the silicone mold, which is compatible with the simplest and least expensive process of autoclaving.

Direct printing of PLA skull cap showed higher mechanical properties, although mechanical behavior of PMMA scenarios is still more than adequate. The "direct print" scenario features a comparable manufacturing time with respect to the "silicone mold" strategy. It also features a complete automation in prosthesis manufacturing. Nevertheless, the high cost of the material and the limitation of the skull dimensions make the "direct print" strategy limited to specific case studies.

The “TPU mold” scenario was the least favorable of the three, particularly in terms of implementation time and sterilization capabilities. Still, a large margin of improvement is expected, related to the choice of a different type of flexible in order to: i) reproject the mold with a lighter structure, ii) exploit alternative sterilization processes. Moreover, the "TPU mold" strategy has a good potential especially in case studies where complex geometries are required.

Statements

All authors have understood the journal's licensing policy.

There are no financial, political, intellectual, religious, or personal relationships between the authors or others that might bias their work.

The manuscript contains original, unpublished work and is not being submitted for publication elsewhere.

This manuscript has been read and approved by all authors, the requirements for authorship have been met, and each author believes that the manuscript represents an honest effort.

The nature of the present study did not require approval by an ethics committee.

References

1. *Low – Cost customized cranioplastiy using a 3D digital printing model: a case report.* A. De La Peña, J. De LA Peña – Brambilia, J. Pérez – De La Torre, M. Ochoa, G. J. Gallardo. 2018, 3D Printing in Medicine, Vol. 4, p. 1-28.

2. *The associated benefits of a cranioplasty on rehabilitation: a review of the literature.* N. Femig, 2020, British Journal of Neuroscience Nursing, Vol. 16, p. 266-271.

3. *Evaluation of implant properties, safety profile and clinical efficacy of patient-specific acrylic prosthesis in cranioplasty using 3D binderjet printed cranium model: A pilot study.* B. Basu, N. Bhaskar, S. B. Vidushi Sharma, S. Das, N. Govindarajan, P. Hegde, P. J. Perikal, M. A. Shivakumar, K. Khanapure, A. T. Jagannatha. 2021, Journal of Clinical Neuroscience, Vol. 85, p. 132 – 142.

4. *A retrospective descriptive study of cranioplasty failure rates and contributing factors in novel 3D printed calcium phosphate implants compared to traditional materials.* M. Koller, D. Trave, G. Shok, S. Murphy, S. Kiaei, U. Samadani. 2020, 3D Printing in Medicine, Vol. 6, p. article number 4.

5. *Autologous Bone Graft: Properties and Techniques.* H. P. Pape, Hans Christoph, A. Evans, P. Kobbe. 2010, Journal of Orthopaedic Trauma, Vol. 24, p. S36-S40.

6. *Interval cranioplasty with patient-specific implants and autogenous bone grafts--success and cost analysis.* B. Lethaus, M. Bloebaum, D. Koper, L. M. Poort-Ter, P.Kessler. 2014 , Journal of Cranio-Maxillofacial Surgery, Vol. 42, p. 1948-1951.

7. *Titanium Allergy: A Literature Review.* M. Goutam, C. Giriyapura, S. K. Mishra, S. Gupta. 2014, Indian Journal of Dermatology, Vol. 59, p. 630-647.

8. *Long-term experience with methylmethacrylate cranioplasty in craniofacial surgery.* D. Marchac, A. Greensmith. 2008, Journal of Plastic, Reconstructive & Aesthetic Surgery, Vol. 61, p. 744–753.

9. *Cranioplasty with polymethyl methacrylate implant: solutions of pitfalls.* A. El-Ghani, M. A. Wael. 2018, Egyptian Journal of Neurosurgery, Vol. 33, a.n. 7.

10. *Complications with PMMA compared with other materials used in cranioplasty: a systematic review and meta-analysis.* R. De Souza Leao, J. Raposo Souto Maior, C. Aparecido De Araújo Lemos, B. Cavalcanti Do Egito Vasconcelos, M. A. Japiassú Resende Montes, E. Piza Pellizer, S. L. D. Moraes. 2018, Brazilian Oral Research , Vol. 32, p. e31.

11. *Reconstruction of Cranial Vault Defect with Polyetheretherketone Implants.* P.Brandicourt, F. Delanoé, F. E. Roux, F. Jalbert, D. Brauge, F. Lauwers. 2017, World Neurosurgery, Vol. 105, p. 783 – 789.

12. *Comparative Cost-Effectiveness of Cranioplasty Implants.* A. Binhammer, J. Jakubowski, O. Antonyshyn, P. Binhammer. 2020, Plastic Surgery, Vol. 28, p. 29-39.

13. *Use of polyetheretherketone (PEEK) in orbital floor fracture reconstruction – A case for concern.* A. Jabar Nazimi, M. Md Yusoff, R.Nordin, S. Nabil. 2015, Journal of Oral and Maxillofacial Surgery, Medicine, and Pathology, Vol. 27, p. 536 – 539.

14. *Customized cost-effective polymethylmethacrylate cranioplasty: a cosmetic comparison with other low-cost methods of cranioplasty.* M. Baldia, M. Joseph, S. Sharma, D. Kumar, A. Retnam, S. Koshy, R. Karuppusami. 2022, Acta Neurochirurgica, Vol. 164, p. 655–667.

15. *Patient specific Polymethyl methacrylate customized cranioplasty using 3D printed silicone moulds: Technical note.* A. Scerrati, F. Travaglini, C. A. E. Gelmi, A. Lombardo, P. De Bonis, M. A. Cavallo, P. Zamboni. 2022, International Journal of Medical Robotics and Computer Assisted Surgery, Vol. 18, p. e2353.

16. *Customized and Cost – Effective 3D Printed Mold for Cranioplasty: India's First Single Center Experience.* S. Gopal, S. Rudrappa, A. Sekar, V. Preethish – Kumar, D. Masapu. 2021, Neurology India, Vol. 69, p. 611 – 617.

17. *Customized Polymethylmethacrylate Cranioplasty Implants Using 3 – Dimensional Printed Polylactic Acid Molds: Technical Note with 2 Illustrative Cases.* J. A. Hay, T. Smayra, R.d Moussa. 2017, World Neurosurgery, Vol. 105, p. 971 – 979.

18. *Surgical results of cranioplasty using three-dimensional printing technology.* Cheng-Hsin Cheng, Hao-Yu Chuang, Hung-Lin Lin, Chun-Lin Liu, Chun-Hsu Yao. 2018, Clinical Neurology and Neurosurgery, Vol. 168, p. 118-123.

19. *Cranioplasty with three-dimensional customised mould for polymethylmethacrylate implant: a series of 16 consecutive patients with cost-effectiveness consideration.* E. Barros Da Silva Júnior, A. H. De Aragão, M. De Paula Loureiro, C. Silva Lobo, A. F. Oliveti, R. Martinelli De Oliveira, R. Ramina. 4, 2021, 3D Printing in Medicine, Vol. 7, a.n. 4.

20. *3D-Printer-Assisted Patient-Specific Polymethyl Methacrylate Cranioplasty: A Case Series of 16 Consecutive Patients.* S. N. Schön, N. Skalicky, N. Sharma, D. W. Zumofen, F. M. Thieringer. 2021, World Neurosurgery, Vol. 148, p. e356-e362.

21. *Customized cranioplasty implants using three-dimensional printers and polymethyl-methacrylate casting.* B. J. Kim, K. S. Hong , K. J. Park , D. H. Park , Y.G. Chung , S. H. Kang. 2012, Journal of Korean Neurosurgical Society, Vol. 52, p. 541-546.

22. *Zauba* [Online] https://www.zauba.com/import-resomer-l-206-s-hs-code.html.

23. *A review of the manufacturing process and infection rate of 3D-printed models and guides sterilized by hydrogen peroxide plasma and utilized intra-operatively.* G. K.H. Shea, K. L. K. Wu, I. W. S. Li, M. F. Leung, A. L. P. Ko, L. Tse, S. S. Y. Pang, K.wan, K. Y. H. Kwan, T. M. Wong, F. K. L. Leung, C. X. Fang. 2020, 3D Printing in Medicine, Vol. 6, a.n. 7.

24. *Additively manufactured medical products – the FDA perspective.* M. Di Prima, J. Coburn, D. Hwang, J. Kelly, A. Khairuzzaman, L. Ricles. 2016, 3D Printing in Medicine, Vol. 2, a.n. 1.

25. *3DP World* [Online] https://3dpworld.it/prodotto/z-support-premium/?gclid=CjwKCAjwwo-WBhAMEiwAV4dybRhbS-905T2kWUG0NZaPZ7BDJiIQ4PAiO5zeYhFt0P-AiSx7xgksExoC1SAQAvD_BwE.

26. *talent* [Online] https://it.talent.com/salary?job=tecnico+informatico.

27. *servizi per utenze* [Online] https://serviziperutenze.it/pun-aggiornamento-dicembre-2020-prezzo-mercato-allingrosso/.

28. *westcmr* [Online] https://www.westcmr.com/43-1280-wb2-43-1280.

29. *Influence of different sterilization processes on the properties of commercial poly(lactic acid).* M. Savaris, V. Dos Santos, R. N. Brandalise. 2016, Materials Science and Engineering: C, Vol. 69, p. 661-667.

30. *Comparative study of different techniques for the sterilization of poly-L-lactide electrospun microfibers: effectiveness vs. material degradation.* A. Rainer, M. Centola, C. Spadaccio, G. Gherardi, J. A. Genovese, S. Licoccia, M. Trombetta. 2010, The International Journal of Artificial Organs, Vol. 33, p. 76-85.

31. *Are the common sterilization methods completely effective for our in-house 3D printed biomodels and surgical guides?* I. Aguado-Maestro, M. De Frutos-Serna, A. González-Nava, A. B. Merino-De Santos, M. García-Alonso. 2021, Injury, Vol. 52, p. 1341-1345.

32. *Evaluation of a Medical Grade Thermoplastic Polyurethane for the Manufacture of an Implantable Medical Device: The Impact of FDM 3D-Printing and Gamma Sterilization.* M. S. M'Bengue, T Mesnard, F. Chai, M. Maton, V. Gaucher, N. Tabary, M. J. García-Fernandez, J. Sobocinski, B. Martel, N. Blanchemain. 2023, Vol. 15, p. 456-469.

33. *CAD generated mold for preoperative implant fabrication in cranioplasty.* J. Wulf, L. C. Busch, T. Golz, U. Knopp, A. Giese, H. Ssenyonjo, S. Gottschalk, K. Kramer. 2005, Studies in Health Technology and Informatics, Vol. 111 , p. 608-610.

34. *Biocompatibility and biomechanical analysis of elastic TPU threads as new suture material.* R. R. Vogels, A. Lambertz, P. Schuster, S. Jockenhoevel, N. D. Bouvy, C. Disselhorst-Klug, U. P. Neumann, U. Klinge, C. D. Klink. 2017, Journal of Biomedical Materials Research. Part B: Applied Biomaterials, Vol. 105, p. 99-106.

35. *A Comprehensive Investigation on 3D Printing of Polyamide 11 and Thermoplastic Polyurethane via Multi Jet Fusion.* W. S. Tey, C. Cai, K. Zhou. 2021, Polymers, Vol. 13, p. 2139-2155.

36. *3D Printed Thermoelectric Polyurethane/Multiwalled Carbon Nanotube Nanocomposites: A Novel Approach towards the Fabrication of Flexible and Stretchable Organic Thermoelectrics.* L. Tzounis, M. Petousis, S. Grammatikos, N. Vidakis. 2020, Materials, Vol. 13, p. 2879-2894.

37. *Is toxicity of PMMA (paramethoxymethamphetamine) associated with cytochrome P450 pharmacogenetics?* M. Vevelstad, E. L. Øiestad, S. Bremer, I. L. Bogen, A. L. Zackrisson, M. Arnestad. 2016, Forensic Science International, Vol. 261, p. 137-147.

Table 1.

Nozzle diameter, mm	0.40
Layer thickness, mm	0.15
Print speed, mm/s	50
Extrusion Temperature, °C	210
Platform Temperature, °C	50
Infill Density, %	20
Fan, %	100
Type Infill	Cube
Raft	Enable
Support material	Z-SUPPORT Premium
Raft enabled	yes
Raft layers	5

Table 2.

Nozzle diameter, mm	0,40±0,01
Layer thickness, mm	0,15
Print speed, mm/s	30
Extrusion Temperature, °C	270
Platform Temperature, °C	90
Infill Density, %	10
Fan, %	Graduate from 0 to 40
Type Infill	Cube
Raft	Enable
Support material	TPU
Raft enabled	yes
Raft layers	5

Table 3.

Printing method / Step timing	Direct print	Two valves silicone mold	Two valves TPU mold
InVesalius 3.1	1 h Of which 40 min specialized computer technician	1 h Of which 40 min specialized computer technician	1 h Of which 40 min specialized computer technician
VxElements	3 h Of which 2h, specialized computer technician and radiology technician	3 h Of which 2h, specialized computer technician and radiology technician	3 h Of which 2h, specialized computer technician *and radiology technician*
Meshmixer	2 h (3 mm thickening) Of which, 10 min of specialized computer technician	3 h (5 mm thickening) Of which, in both cases, 10 min of specialized computer technician	2 h (3 mm thickening) Of which 10 min, specialized computer technician
SolidWorks	-------	-------	• Upper valve: 8 h; • Lower valve: 6 h All active projecting time (specialized computer technician)
Z-Suite	1 h Of which, 1h of specialized computer technician	---------	• Upper part: 15 min • Lower part: 15 min All active projecting time (specialized computer technician)
Simplify3D software	-------	1 h Of which, 1h of specialized computer technician	----
Total	7 h	8 h	20 h 30 min

Table 4.

STL file	7 h
Printing time	22 h 47 min
(+extra time of printing step)	30 min
Total	30 h 17 min

Table 5.

STL file	8 h
Printing time	9 h
(+extra time of printing step)	30 min
Hand manufacturing of two valve mold	1 h
Drying time of medical-grade silicone elastomer at R.T.	20 min
PMMA pouring	5 min
PMMA drying	10 min
Total	19 h, 5 min

Table 6.

STL file (total value, upper and lower valve)	20 h 30 min
Printing time	• Upper valve: 2 G 7 h 18 min • Lower valve: 1 G 18 h 32 min
(+extra time of printing step)	• Upper valve: 30 min • Lower valve: 30 min
PMMA pouring	5 min
PMMA drying	20 min
Total	119 h 45 min

Table 7.

	Direct print orthogonal	Direct print parallel	TPU mold orthogonal	TPU mold parallel	Silicone mold orthogonal	Silicone mold parallel
Thickness	3.30±0.04	3.16±0.01	3.3±0.1	3.18±0.06	2.85±0.1	2.9±0.2
Δ %	9.95	5.27	9.83	6.11	-5	3.3%
Width	13.1±0.4	12.9±0.01	12.5±0.1	12.5±0,2	12.51±0.1	12.6±0.2
SD %	3.26	1.84	-1.30	-1.81	-1.50	0.8 %
Length	128.0±0.3	126.8±0.2	125.50±0.5	124.3±0.9	127.95±	123.7±
SD %	0.76	-0.17	-1.19	-2.09	0.75	2.6 %

Table 8.

Sample	**(Ra ± s.d) µm**
Direct print - orthogonal	19.29±0.08
Direct print - parallel	18.7±0.1
TPU mold - orthogonal	37±2
TPU mold - parallel	42±2
Silicone mold - orthogonal	2.23±0.09
Silicone mold - parallel	2.9±0.1

Table 9.

Scenario	**Flexural Modulus, MPa**
Direct print - parallel	2974 ± 5
Direct print - orthogonal	2300 ± 200
TPU mold - parallel	2200 ± 100
TPU mold - orthogonal	1400 ± 200
Silicone - mold parallel	1700 ± 200
Silicone - mold orthogonal	1700 ± 200

Patient specific customized cranioplasty by 3D printing of biopolymers, 3D printed molds and silicone molds.

Flora B[1-2], Scerrati A[3,4], Trovalusci F[5], Vesco S[5]

[1]Department of Clinical Sciences and Medicine, University of Rome "Tor Vergata", Rome, Italy
[2]CIMER, Interdepartmental Centre for Regenerative Medicine, University of Rome "Tor Vergata", Rome, Italy
[3]Neurosurgery, Sant'Anna University Hospital Ferrara, Ferrara, Italy;
[4]Department of Translational Medicine, University of Ferrara, Ferrara, Italy;
[5]Department of Enterprise Engineering, University of Rome "Tor Vergata", Rome, Italy.

Abbreviations

ABS: Acrylonitrile Butadiene Styrene
AM: Additive Manufacturing
BVOH: Butenediol Vinyl Alcohol Copolymer
CT: Computed Tomography
FDM: Fused Deposition Modelling
HPGP: Hydrogen Peroxide Gas Plasma
PEEK: (poly ether ether ketone)
PLA: Poly Lactic Acid
PMMA: Poly(methyl methacrylate)
TPU: Thermoplastic Polyurethane

Keywords: Bone, craniofacial, reconstruction, additive manufacturing, prosthetics, patient-customized prosthesis, implantable FDM filament, medical-grade materials.

Abstract

With the advancement of 3D printing technologies, the possibility of manufacturing patient-specific cranioplasty has emerged as an alternative to autologous bone.

In this study, three different strategies using fused deposition modelling (FDM) additive manufacturing (AM) were applied and compared: (i) direct printing of PLA (polylactic acid) prosthesis, mold casting of poly(methyl methacrylate) (PMMA) prosthesis using (ii) silicone mold, (iii) thermoplastic poly urethane (TPU).

All techniques studied achieved good geometric accuracy and cosmetic appearance.

Direct printing of the PLA prosthesis resulted in the fastest strategy, followed by PMMA casting in silicone mold. Nevertheless, the use of silicone mold led to many advantages, such as lower costs and the possibility of using autoclaving as a sterilization technique.

1. Introduction

In the craniofacial region, trauma and tumors are common pathologies that may require the restoration of a small or large amount of osteocartilaginous tissue. In cranioplasty procedure, the replacement of the missing bone has a positive influence on both physical and neurological state of the patient, leading to reduction of healing time, preservation of the underlying brain and improvement of the patient's appearance (1) (2).

This clinical procedure usually involves the use of prostheses made of various materials, allogenic or not, such as titanium (Ti), ceramic, polymeric or transplanted bone materials (3) (4). In some cases, the primary tissue for cranioplasty is autologous bone (5) (6). However, this strategy is limited by the potential for bone resorption.

Titanium has anti-inflammatory and non-corrosive properties, but may cause an increase in hypersensitivity due to prolonged and continuous exposure to this metal (7). The most popular implantable polymers are PEEK (polyetheretherketone) and PMMA (8) (9).

In particular, PEEK shows excellent implant success due to its high biocompatibility, although the risk of prosthesis rejection is not completely eliminated (10). It has excellent mechanical resistance and is easy to machine (11). However, PEEK polymer is not the standard choice for cranioplasty due to the high cost of material and processing equipment (12). In addition, the lack of radiopacity of PEEK may interfere with the radiologic imaging technique used to evaluate prosthesis placement (13). PMMA is the most widely used polymeric material for cranioplasty, offering the best compromise between mechanical properties, biocompatibility and cost. PMMA exhibits high mechanical resistance at compression, good heat resistance (3), and leads to a higher rate of infection (10).

Both PEEK and PMMA are suitable for 3D printing. (14). This customizable manufacturing process has emerged in recent years in medicine for its potential in creating patient-specific prostheses.

A missing part of a bone is replicated by processing a high-resolution computed tomography (CT) scan of the head with appropriate CAD software (15). The use of a native model greatly improves the quality of the prosthetic design (16).

The prosthetic system can be prefabricated or fabricated during the preoperative phase using 3D printers (17), reproducing the patient's specific skull geometry previously determined by CT (18).

However, the cost of industrial and commercial 3D printers has kept 3D printing from being widely adopted.

In recent years, the introduction of desktop 3D printers has lowered the cost of these machines (17); on the other hand, 3D printing of custom molds (mono- or bi-valves) has emerged as an alternative process to direct 3D printing of a cranial flap with thermoplastic filament (19).

This alternative strategy allows the use of non-printable polymeric materials, such as liquid medical grade PMMA oligomer. The technique consists of directly printing a mold using a thermoplastic filament, such as PLA. The thermoplastic material can be chemically inert and medical grade to create a mold that can be used in direct contact with the liquid oligomer used for casting (e.g. PMMA) (18). Alternatively, a low-cost non-medical material can be used for printing by covering the mold with special sterile plastic bags (e.g., surgical incision drape (17), silicone layer (19)). However, special attention must be paid to the choice of the cover material, since the exothermic phase of polymerization of the cast oligomer may affect the surface of the bag, leading to partial dissolution and release of chemicals (20).

Another aspect to consider in the casting strategy is the assessment of skin contracture prior to implant design (21). Finally, the cast mold models may require post-processing adjustments related to the coupling of bi-valve molds (17) (20).

The present study will provide a comparison between three main strategies for AM fabrication of cranial prostheses: direct 3D printing of prostheses, use of a 3D printed rigid mold, and use of a soft mold obtained from a 3D printed bone master.

2. Materials and methods

2.1 DICOM files processing

The three techniques presented here for the realization of a patient-specific prosthesis all share a common procedure for the elaboration of the model, which represents the first step of the methods. This is the acquisition of the anatomy of the patient's skull, prior to the decompressive craniotomy, by CT and its storage as DICOM files. The DICOM files are processed by using, in sequence, the software InVesalius 3.1, VxElements, Meshmixer, Simplify3D.

InVesalius, version 3.1, (Invesalius, Brazil) is an open source software used to translate DICOM files into 3D image files. The software is programmed for the reconstruction of computed tomography and

magnetic resonance images and their advanced 3D visualization. The software is equipped with image segmentation and measurement tools.

VxElements (Ametek Creaform, Italy) is an open source, post-processing, scan-to-CAD software module to be integrated with the use and design of CAD software. Vx Element is designed for the optimization of the mesh: here has been used to remove fictive structure errors.

The output files, consisting of 3D images of a surface, are then processed by Meshmixer 3.5 software to perform thickening. Meshmixer is a state-of-the-art, open-source software for working with triangular meshes, published by Autodesk Ireland Corporation UC, Ireland. The prosthesis models were then thickened with different values depending on the final implementation technology. Direct printing of the prosthesis required a model thickness of 3.00 mm (i.e., the average dimension of the original cranial bone). The same model was used to project the TPU mold. The master model used to shape the silicone mold was designed with a thickness of 5.00 mm. The larger space in the lumen of the mold was provided taking into account the space required for the allocation of the upper valve of the mold (lid).

A second meshing using Meshmixer completes the process to reduce the degree of error that may occur during thickening operations.

Prior to direct printing of the PLA cranial flap, the file from Meshmixer is processed using Z-Suite (Zortrax Software, Zortrax S.A., Poland) to perform slicing, set the orientation of the model, and position the pillars and supports.

In the procedure that includes the production of the silicone mold, the file in the output of Meshmixer is processed by the open source software Simplify3D, version V4 (Simplify 3D; Italy). This is a specific software compatible with the use of Delta printers (see section 2.2.2) and designed for the slicing process and other operations that precede the printing step. In fact, in the same phase, the printing orientation and the positioning of the columns are added to the model using the same software. An orientation with the concavity facing down is set.

In the development of two-valve, TPU mold method, the designs of the two half of the molds, superior and inferior, is carried out processing the model by using SolidWorks software (Dassault Systèmes, France), and Z-Suite in sequence, to return two separate .zcode files. In this case, Z-Suite is also used to perform the slicing process instead of Simplify3D software.

All the STL files have been projected, oriented and optimized for the shortest printing time.

2.2 Cranioplasty implementation

2.2.1 3D direct printing of biopolymers

Direct printing of the cranial portion identified for the implementation of the prosthesis was performed using the STL file described in Section 2.1. A non-implantable medical grade PLA

filament was selected to proceed with the printing feasibility studies. Namely, PLA bone Healthfil (Treed Filaments, Seregno (MB), Italy), was chosen because of its mechanical properties and texture, which accurately reproduce the behavior of natural bone. The printing process was performed using a Zortrax M300 Dual FDM printer. The processing parameters are shown in Table 1.

Table 1: Operative parameters for the printing process of PLA filament

2.2.2 PMMA casting by silicone molds

Silicone molds were realized by a specific company of 3D printing (CAD Ortopedia, S.r.l., U.s., Ganzanigo, BO). The mold was made using as a master an ABS (Acrylonitrile Butadiene Styrene) printed model of the missing cranial flap. The master was obtained by 3D printing an ABS filament (Wasp S.r.l., Italy) using a nozzle temperature of 220 °C, a bed temperature of 55 °C, a standard printing speed of 45 mm/s, a x/y axis movement speed of 150 mm/s, and a z axis movement speed of 150 mm/s. The film thickness was set to 0.15 mm.

An industrial printer, Delta Wasp 4070 (Wasp S.r.l, Italy), was used in the process (15). Figure 1 shows the image of the 3D printed master in ABS.

Figure 1 3D-printed master in ABS of the cranial flap.

The silicone mold was composed of 2 complementary pieces. A 1 cm diameter hole was left at the highest point of the mold profile to allow the poured PMMA (Cranioplastic, Codman& Shurtleff, inc., USA) to complete filling of the mold. A schematic illustration of the mold is shown in Figure 2.

Figure 2 Schematic representation of the silicon mold during the phase of cranial flap extraction

2.2.3 PMMA casting by 3D printed TPU molds.

The 3D printing of the two valves was performed using an elastic TPU filament (Elasto A, Treed Filaments, Seregno (MB), Itay). A Zortrax M300 Dual printer (Zortrax S.A., Poland) was used for the additive manufacturing process. The processing parameters defined using the corresponding Z-Suite 2 (version 2.23.0) slicing software (printer software, Zortrax S.A., Poland) and tested in preliminary studies are shown in Table 2.

Table 2 Operative parameters in the printing process of two valves mold using TPU filament

Liquid PMMA (Cranioplastic, Codman& Shurtleff, inc., USA) was then poured into the TPU mold through the hole at the top, following the procedure described in 2.2.2.

2.3 Characterization

The mechanical properties of skull tops and their dependence on the printing direction of: the prosthesis ("direct print" strategy), the master ("silicone mold" strategy), or the mold ("TPU mold" strategy), were evaluated by flexure tests.

The test specimens were obtained by controlling the printing direction, which is considered to be the direction of growth of the deposited layers. Two main axes were considered: "parallel" axis (or direction) consists in the axis that runs parallel to the plane where a deposited filament lies, "orthogonal axis" runs parallel to the growth direction of the layers.

Rectangular samples were obtained in the two directions, with dimensions of (127.00 x 12.70 x 3.00) mm, according to ASTM D790 standard, for each of the three fabrication approaches.

Specimens obtained by direct 3D printing of PLA were implemented so that their growth direction was parallel or perpendicular to the longest edge of the disc (Figure 3). STL file of the samples is shown in (Figure 3-a and Figure 3-b). The blue arrow indicates the growth direction of the layers. Printing conditions and materials are the same as described in section 2.2.1.

Figure 3 "Direct print"scenario: STL files file of a) parallel and b) orthogonal samples; c) printed samples in the two orientations

Rectangular specimens, representative of the scenario of PMMA casting through silicone molds, were prepared following an operational procedure analogous to that described in section 2.2.2. ABS masters of the rectangular specimens required for the silicone mold were printed using the same orientation adopted for the PLA disks (same STL file reported in Figure 3). The printing conditions were the same as for ABS reported in 2.2.2. ABS discs were immersed in a silicone pot. After the silicone was cured (Figure 4-a), the ABS specimens were manually removed. Sockets formed by ABS discs were then filled with liquid PMMA. After curing, PMMA disks characterized by two orientations, orthogonal and parallel, were removed (Figure 4-b).

Figure 4 "silicone mold" scanario: a) preparation of silicone mold with ABS masters; b) cast samples in the two orientations.

STL files of TPU molds for PMMA casting, along the two directions, are reported in (Figure 5-a, Figure 5-b). The growth direction of TPU filament deposition is indicated by the blue arrow reported in the figure, where mold cavities are also visible. Nevertheless, the mold cavities were implemented with rectangular geometry of (127.00 x 12.70 x 3.00) mm dimension.

Figure 5 "TPU mold" scenario: STL file of a) parallel mold and b) orthogonal mold; c) cast samples in the two orientations

Slices obtained after PMMA casting and curing are shown in Figure 5-c.

Bending property tests were performed on the above disks in accordance with ASTM D790.

The finish of the samples was analyzed using an inductive profilometer (TalySurf CLI 2000, Taylor Hobson, Leicester, UK) to evaluate the influence of the manufacturing strategies on the texture of the outer surface. An area of 4x4 mm2 was scanned with a resolution of 1 mm to evaluate the roughness parameters and to construct the corresponding 3D maps. Data processing was performed using TalyMap 3.1 software (Taylor Hobson, Leicester, UK).

Dimensional accuracy was determined on each dimension (thickness, width, length) using Equation 1:

Eq. 1 $\Delta\ \% = \frac{(D_p - D_a)}{D_p}\ 100$

Where:

$D_p =$ Dimension provided by the project (thickness/width/length)

$D_a =$ Average dimension (thickness/width/length)

Dimensions were determined by caliper measurement (Z22855F, OWIM GmbH & Co., Germany).

The energy consumption associated with the manufacturing process was evaluated by measuring the electrical energy consumed during the printing process using a plug-in power meter socket (model PM01, Maxcio, China).

3. Results

3.1 DICOM files processing

High-resolution CT scans of the preoperative patient's skull were performed and processed to obtain the STL file for reconstruction of the defected area after surgery. In this way, the elaboration of the DICOM file did not require any processing of virtual reconstruction of the missing bone (mirroring of the whole skull section, opposite to the removed section, interpolation or graphical restoration).

The results of DICOM file processing are shown in Figure 6. In particular, Figure 6-a shows the output image immediately after processing by VxElement, where a 3D image is created and fictive structures are removed, where the spikes or lumps are removed. The latter image, when imported and opened with Meshmixer, appears in Figure 6-b. The image shows an irregular mesh (automatically applied by the software) of a 2D surface with no thickness applied. Some errors created during the file import were removed in the same step, as can be seen in the magnification. The imported file was then processed by Meshmixer to obtain a thickening of 3 mm or 5 mm, depending on the

manufacturing method. After thickening, a second meshing procedure was applied to remove errors from the thickening step (Figure 6-c).

Figure 6: Images of a selected section of patient's cranium, selected as model for the implant manufacturing: a) 3D model of cranium surface; b) same surface after meshing process; c) model after thickening and the second step of meshing.

The images were then ready to be processed to perform the slicing step, set the printing orientation of the skull cap, and design the supports and pillars.
Direct printing of the PLA cap requires the Z-Suite software to perform slicing as it is compatible with the Zortrax M300 Dual FDM printer (Figure 7).

Figure 7 Slicing file of 3 mm PLA skull cap.

The design of the TPU mold was performed by processing the Meshmixer output file using SolidWorks software. In this step, the structures of the two valves of the mold were designed (Figure 8-a). As for the PLA cap, the TPU mold design file was sliced and adapted to the printing step using Z-Suite (Figure 8-b).

Figure 8 3D image of a) upper mold half (left) in upside down position, and lower mold half (right) in upside down position; b) slicing files of structures as in a)

The elaboration process, from DICOM to printing the STL file, was shared among the three manufacturing methods. However, the process time for the realization of the 5 mm ABS master was longer due to the higher number of iterations performed in a thicker model. In addition, the TPU bi-valve mold required additional time due to the SolidWorks projection of the mold. Also, mesh refinement and slicing procedures were required to process both files using Z-Suite software.
The slicing and image processing procedures were performed by a specialized computer technician and a radiology technician. The different steps of a standard case in which no noise or anomalies were found, and the personnel involved in each step, are shown in Table 3.

Table 3 Step timing, men hours and software used for the elaboration of each step from DICOM file to printing file

3.2 Biopolymer cranioplasty

An image of the resulting cranial flap is shown in Figure 9. The images show the use of two different materials: one for printing the skull prosthesis (PLA, non-implantable medical grade), the second for

the realization of the raft and the pillars (butenediol vinyl alcohol copolymer (BVOH)_Z-Support Premium, which is compatible with PLA).

This choice was made intentionally to reduce the cost of the materials. In fact, the implantation implies the change from medical grade PLA filament (used in this study) to implantable grade PLA filament. The amount of BVOH consumed for the deposition of the supports was 17.02 g, which represents approximately 43% of the total material consumed in the printing, being the amount of PLA consumed for the cranial flap of 45.02 g. This represents a significant savings since the cost of implantable PLA is reported to be 82.72 per gram (22), while the cost of an 800 g package of support filament was 119.00 € (23). In these quotes, the total price for the materials used in the printing (both PLA and BVOH) was 3724.00 €.

The use of a non-implantable polymer in contact with the implantable prosthesis has been reported in the literature (24) and has been shown not to affect or contaminate the medical quality of the implant when subjected to prior thorough washing (25).

However, the same model can be printed entirely in implantable grade PLA, without significant modification to the printer setup, and still at a reasonable cost (5132.00 €) (23).

Figure 9 Cranial flap obtained from direct printing of PLA filament

The printing time for the realization of the PLA prosthesis takes a total time of 30 h 17 min. This includes the time for segmentation of the DICOM file, the slicing of the STL files, the study and adjustment of the model supports (columns), which takes an average time of 7 h. The average time for printing the results is 22 h 47 min, with an "extra time" of 30 min to be added. The extra time defines the setup of the filaments and the printer, the time for removing the model from the machine and the removal of the supports, all parameters that depend on the operator.

Use of personnel, in accordance with Table 3, including extra time operations, affects the cost of direct printed prosthetic with an intake of 98.49 €. Costs per hour for radiology technician and a PC specialized technician were obtained from talent.com (26).

The total cost of one hour of PC work, including energy consumption and depreciation, was 0.2287 €/h, then 1.60 € for the entire design and cutting of the PLA prosthesis. PC depreciation per hour was calculated on the basis of a two-year lifetime, considering 220 working days per year, a working day of 8 h, with an average initial cost of 800 €. PC energy consumption per hour was measured at 0.013 KWh, with an energy cost of 0.1249 €/KWh, related to PUN value in 2020 (27).

Printing time contributes with a "machine time cost" of 21.9 € for the PLA skullcap. The price includes machine depreciation, from an average initial cost of 4000.00 € (0.91 €/h with 20 hours per

day of unattended working time, for 220 days per year) and energy consumption (0.19 KWh for printing set-up of PLA).

In conclusion, the total cost for the implementation of PLA skullcap was of 5253.99 €.

Table 4 shows the timing of the printing process.

Table 4 Timing in manufacturing process of PLA skull flap by direct printing

3.3 Silicon mold

The silicone molds were made by a specialized external supplier (Cad Ortopedia S.r.l., Ganzanigo (BO), Italy). The total manufacturing time, from master printing to silicone mold forming, was 10 h 50 min. In this way, the process, from conversion of DICOM file to mold achievement takes 23 h and 25 min, while the total manufacturing time, including PMMA coping preparation, resulted of 19 h (Table 5).

Table 5 Timing in manufacturing process of PMMA skull flap by silicone mold

The total cost of the silicone mold was 2700.00 €. This price includes the cost of a single dose of PMMA (330.00 € (28)). Within a certain range (from 1 g to the size of the sterilized package), the cost of PMMA does not really vary, since once the sterilized dose is opened, the excess material must be disposed of. The total cost of the prosthesis was therefore 3030.00 €. The resulting cranial flap is shown in Figure 10.

Figure 10 PMMA cranial flap obtained from silicone mold (15)

For comparison purposes only, the data provided by the company was used to prepare a quotation as if the same method were carried out with the same printer, equipment and personnel as for the other two methods. In this regard, according to Table 3, the cost of personnel was 110.47 €, the cost of equipment was 1.83 € for the PC and 8.5 € for the printer, taking into account depreciation and energy consumption, and the total cost of materials (medical ABS for the model, medical silicone for the mold, implantable PMMA) was 380.61 €. The total cost of the prosthesis was 501.43 €, much lower than the commercial cost.

3.4 TPU mold

Image of two valve mold is reported in Figure 11, Figure 12, and Figure 13.

Figure 11 Views of upper mold half of printed TPU mold.

Figure 12 Views of lower mold half of printed TPU mold.

Figure 13 Views of two valves mold of printed TPU mold.

The timing of each step of the process is shown in Table 6.

Table 6 Timing in manufacturing process of PMMA skull flap by TPU mold

From the values reported in Table 3 and Table 6, the printing phase was the most time-consuming step for this method. It took 1 D 18 h 32 min to print the lower valve of the mold and 2 D 7 h 18 min for the upper part, for a total of 4 D 1 h 50 min. Extra time of 30 min was considered. The total extra time of 1 hour is considered to include the PMMA casting and prosthetic extraction step.

The registered energy consumption per hour in the printing process of TPU was 0.2780 KWh, which is higher than that of PLA or ABS because it requires more energy due to the higher temperature applied. Including the depreciation of the printer of 0.91 € per hour, the total cost of the printing process of the upper and lower mold halves was 92.35 €. Contribution to the cost of PC usage was also higher due to longer elaboration times related to the design and implementation of two molds, with a total expenditure of 4.60 €.

Similarly, personnel costs increased up to $299.95, according to Table 3.

In the post-processing phase, the amount of material used was quantified and this value was used to calculate the cost of this scenario. Specifically: 208.64 g were used to print the upper mold, including raft and supports, while 186.20 g were used to print the lower mold half. Since the cost of the filament was 41.00 € for a 0.5 kg package (i.e. 0.08 €/g), the final cost was 32.38 €. To this cost must be added the price of medical grade PMMA, which contributes to the total cost of 330.00 € (28). Then, the total cost of a prosthesis obtained by TPU casting is of 759.28 €.

3.5 Characterization of skullcaps

Surface roughness and mechanical properties were evaluated to understand the effect of processing technology and processing direction on patient-specific skull caps.

First, the geometric accuracy of the specimens was evaluated.

Table 7 Dimensional accuracy of samples of the three scenarios, obtained in the two main orientations.

Depending on the manufacturing strategy, and processing direction, the sample finishing differs each other, even significantly (Figure 14, Table 8).

Figure 14 Morphological maps under adapted scale (from a) to f) plots) and normalized scale (from a') to f') plots) of slab samples obtaine by: a), a') parallel and b), b') orthogonal PLA direct print; c), c') parallel and d), d') orthogonal silicone mold; e, e') parallel, f), f') orthogonal TPU mold.

Table 8 Arithmetic average height values (Ra) of slabs samples obtained by the three different strategies along the two orientations

Ra values range from the lowest, 2.9 and 2.23 µm, found in the "silicone mold" scenario, to 42 and 37 µm, found in the "TPU mold" scenario. The direct print samples showed Ra values in the middle, with values of 18.7 and 18.22 µm. The influence of the processing direction is reflected in the Ra differences between the corresponding samples. Δ values range from -0.59 µm in "direct print" to a maximum of 5 µm in "TPU mold" scenario. The Ra values in the "direct print" scenario are quite similar in both directions because the surface texture is mostly related to parameters such as filament diameter, infill, spacing, etc. The "silicone mold" scenario also shows a moderate Δ of 0.67 µm, which is also the smoothest sample in this study.

This reflects the mechanical behavior of a soft but fragile material such as silicone, from ribs or notches, contextual to the ABS master removal from the mold, even in a favorable configuration, such as parallel configuration. On the other hand, a combination of elements, such as the high viscosity of uncured PMMA, the local flexibility of silicone and an unfavorable wettability, partially hides the complexity of the printed texture. Nevertheless, the mold thickness is sufficient to ensure the correct shape of the sample.

This reflects the mechanical behavior of a soft but fragile material such as silicone, which loses ribs and notches when the ABS master is removed from the mold, even in a favorable configuration such as parallel. On the other hand, a combination of elements, such as the high viscosity of uncured PMMA, the local flexibility of silicone and an unfavorable wettability, partially hides the complexity of the printed texture. Nevertheless, the mold thickness is sufficient to ensure the correct shape of the sample.

Table 9 Flexural modulus of slabs samples obtained by the three different strategies along the two orientations

Figure 15 Load-displacement curves for flexural tests

In order to compare the influence of filament orientation, a displacement of 3.76 mm was chosen to calculate the differences in load values between the parallel scenarios and the corresponding

orthogonal samples. This value was chosen because it was found to be the average displacement at break achieved by the "direct print - orthogonal" specimen.

The highest mechanical strength was exhibited by samples obtained by direct printing of PLA filament in both directions. "Direct print - orthogonal was found to be the only sample with breakage. A 71.01 N difference in sample response was measured at the set deformation. This scenario resulted in the most network-dependent results, as the filament orientation influences the mechanical properties through most of the sample thickness. In this way, the effect of the parallel oriented filament as a reinforcing rib or the notch occurring between the orthogonally oriented filaments are even more pronounced.

The flexural modulus values of the PMMA specimens produced through the TPU mold are lower than the values registered for the first scenario (direct printing, both orientations). A difference of 22.72 N was found between the two orientations.

Both parallel and orthogonal orientations of the silicone mold scenario showed the lowest flexural modulus. In this scenario, the influence of orientation was negligible because the load is intercalated against the displacement curves. This behavior was probably due to the smoother surface of the specimens (Figure 14), which does not represent a reinforcing rib or notch.

In addition to the influence of the printing direction, the sample material was identified as the most important factor influencing the mechanical properties. This aspect would be even more true (under the same infill and model conditions) when implementing a patient-specific prosthesis, since changes in filament orientation are gradual and intertwined when manufacturing a cupped geometry. The stresses applied to this intricate network partially compensate for each other.

3.6 Sterilization process

The sterilization process is a critical step for the success of implantation surgery. In particular, in addition to removing all colony forming u nits, the process used must not induce degradation or release of toxic substances from the treated surface.

An analysis of the relevant literature identified Hydrogen Peroxide Gas Plasma (HPGP) (29) (30) as a suitable sterilization technique for medical grade PLA, while the use of the traditional autoclave is limited to particularly resistant geometries (for cylindrical shape, a diameter greater than 5 mm) (31). HPGP undergoes a sterilization cycle at 45 °C for 45 min.

Platinum-cured liquid silicone rubber, the specific material widely used in healthcare products due to its stability and inertness, can be safely sterilized in many different ways: autoclave, dry heat or gamma irradiation. In this specific case study, an autoclave cycle of 1 hour at 134°C and 2.7 bar was applied.

Sterilization of TPU filaments has been tested in the literature and has been shown not to alter the biocompatibility of the material in terms of cytotoxicity, nor the mechanical and geometric properties of the phantom (32). This was done using the gamma radiation sterilization method. An irradiation of 40 KGy, according to ISO 11137-2. This irradiation is achievable through a variable time, depending on the minimum intensity of the radiation and processing conditions. The process, usually applied in continuous, can last from hours to days.

4. Discussion

The comparisons between the three methods under analysis are discussed below.

The first aspect considered is the cost of production of the skullcaps.

Direct printing of a PLA skullcap would cost 5254 €. The high cost is mainly due to the implantable PLA filament. The costs of the "silicone mold" and "TPU mold" scenarios were significantly lower, with a current cost of 501 € and 759 €, respectively.

In terms of mechanical resistance, all orientations of the "direct print" and "TPU mold" scenarios showed values of flexural modulus close to, or higher, than both the orientations of the "silicone mold" scenario. Nevertheless, this latter scenario was considered as a reference because the specimens were obtained by a technology already successfully used in clinical practice. The use of direct printing of PLA improved the hardness and flexural stiffness of samples, reaching values up to (2974 ± 5) MPa for parallel orientation, while "silicone mold" - orthogonal samples collapsed in a range of applied stresses from around 5 to over 8 MPa. In these terms, the mechanical behavior of PMMA-containing scenarios, even if characterized by lower rigidity, can be considered "more resilient" for the application selected, since no specific orientation induces fragile behavior.

Implementation time was analyzed considering all steps from the slicing of the DICOM file to the post-processing of the printed skull cap. The processing time was approximately in the same order of magnitude as reported for PLA “direct print” technology and “silicone mold technology”, being 30 h 17' and 19 h 5', respectively. This time was recorded despite the inclusion of some additional steps, namely the manufacturing step of the silicone mold, and PMMA casting and drying. This finding was due to the combination of two elements: the ease of printing ABS compared to PLA filament, and the use of a more expensive/sophisticated printer in the silicone mold scenario. Technology using TPU printed molds, took significantly longer time, 119 h 45', due to the presence of two mold halves to be printed and elaborated.

Since sterilization step is considered, the possibility of using autoclave on silicone mold makes this technology of choice. In fact, autoclave is the most economical strategy, both in terms of initial investment and running costs, compared to gamma irradiation or the HPGP method. Autoclave sterilization and HPGP also have a comparable treatment time (1 hour vs. 45 minutes, respectively).

On the other hand, gamma irradiation, the only strategy currently tested and found to be inappropriate for the sterilization of TPU filament, resulted in (32). This technique, although very effective also in the weft of the printed piece, has several drawbacks, including long treatment times (from hours to days), management of radioactivity and, consequently, high costs.

Direct printing of PLA prostheses has a good potential for standardization in terms of minimizing operator-dependent variability. The printing phase provides a part with a fairly reliable profile compared to the original model.

A second method for the realization of a cranial prosthesis considers the production of a silicone mold. The design of the printing model does not really require any modification, since silicone molds are made by hand on a master printed in ABS, following a procedure that is completely analogous to the direct printing of the PLA prosthesis. The preparation of the silicone mold is done manually, therefore it takes some time and its quality depends on the operator.

The "TPU mold" strategy differs from the previous two since the CT image processing and file elaboration involves the design of a separate file for each of the two valves of the mold. This step requires the intervention of an operator whose ability depends on the efficiency of the mold, the amount of TPU filament consumed and the printing time. Nevertheless, for this method, the intervention of operator in the manufacturing of molds is not required as for the silicone mold, specifically in the mold manufacturing step. This provides the "TPU mold" method with a higher potential of automation, as the main advantage over the use of silicone mold.

PMMA implants have a biocompatibility and induce an inflammatory that are more compatible, compared to PLA, with the implementation of large-size implants. Nevertheless, the implantation of PMMA prosthesis require to ensure the complete polymerization of PMMA to avoid the exposure of neural tissue to the heat generated during polymerization (21), or the contact with unreacted chemicals. In this scenario, casting is the critical step. The mold could be realized in silicone or in TPU, and these materials are both good choices (33). Although the release of traces of TPU during polymerization of PMMA needs to be evaluated in future studies, a review of the relevant literature suggests that TPU is a material with a reduced induction of inflammatory response (34).

Conclusions

Three procedures were discussed here for the implementation of cranioplasty. Among these three, the "silicone mold" scenario presented the highest number of beneficial, according to most of the evaluation criteria considered. In particular, the possibility of using implantable PMMA for the manufacture of the skullcap, a material that features a lower inflammatory response, as a higher compatibility, with respect to PLA. Implantable PMMA is supplied as a sterile product, so the only

part that needs to be sterilized is the silicone mold, which is compatible with the simplest and least expensive process of autoclaving.

Direct printing of PLA skull cap showed higher mechanical properties, although mechanical behavior of PMMA scenarios is still more than adequate. The "direct print" scenario features a comparable manufacturing time with respect to the "silicone mold" strategy. It also features a complete automation in prosthesis manufacturing. Nevertheless, the high cost of the material and the limitation of the skull dimensions make the "direct print" strategy limited to specific case studies.

The “TPU mold” scenario was the least favorable of the three, particularly in terms of implementation time and sterilization capabilities. Still, a large margin of improvement is expected, related to the choice of a different type of flexible in order to: i) reproject the mold with a lighter structure, ii) exploit alternative sterilization processes. Moreover, the "TPU mold" strategy has a good potential especially in case studies where complex geometries are required.

Statements

All authors have understood the journal's licensing policy.

There are no financial, political, intellectual, religious, or personal relationships between the authors or others that might bias their work.

The manuscript contains original, unpublished work and is not being submitted for publication elsewhere.

This manuscript has been read and approved by all authors, the requirements for authorship have been met, and each author believes that the manuscript represents an honest effort.

The nature of the present study did not require approval by an ethics committee.

References

1. *Low – Cost customized cranioplastiy using a 3D digital printing model: a case report.* A. De La Peña, J. De LA Peña – Brambilia, J. Pérez – De La Torre, M. Ochoa, G. J. Gallardo. 2018, 3D Printing in Medicine, Vol. 4, p. 1-28.

2. *The associated benefits of a cranioplasty on rehabilitation: a review of the literature.* N. Femig, 2020, British Journal of Neuroscience Nursing, Vol. 16, p. 266-271.

3. *Evaluation of implant properties, safety profile and clinical efficacy of patient-specific acrylic prosthesis in cranioplasty using 3D binderjet printed cranium model: A pilot study.* B. Basu, N. Bhaskar, S. B. Vidushi Sharma, S. Das, N. Govindarajan, P. Hegde, P. J. Perikal, M. A. Shivakumar, K. Khanapure, A. T. Jagannatha. 2021, Journal of Clinical Neuroscience, Vol. 85, p. 132 – 142.

4. *A retrospective descriptive study of cranioplasty failure rates and contributing factors in novel 3D printed calcium phosphate implants compared to traditional materials.* M. Koller, D. Trave, G. Shok, S. Murphy, S. Kiaei, U. Samadani. 2020, 3D Printing in Medicine, Vol. 6, p. article number 4.

5. *Autologous Bone Graft: Properties and Techniques.* H. P. Pape, Hans Christoph, A. Evans, P. Kobbe. 2010, Journal of Orthopaedic Trauma, Vol. 24, p. S36-S40.

6. *Interval cranioplasty with patient-specific implants and autogenous bone grafts--success and cost analysis.* B. Lethaus, M. Bloebaum, D. Koper, L. M. Poort-Ter, P.Kessler. 2014 , Journal of Cranio-Maxillofacial Surgery, Vol. 42, p. 1948-1951.

7. *Titanium Allergy: A Literature Review.* M. Goutam, C. Giriyapura, S. K. Mishra, S. Gupta. 2014, Indian Journal of Dermatology, Vol. 59, p. 630-647.

8. *Long-term experience with methylmethacrylate cranioplasty in craniofacial surgery.* D. Marchac, A. Greensmith. 2008, Journal of Plastic, Reconstructive & Aesthetic Surgery, Vol. 61, p. 744–753.

9. *Cranioplasty with polymethyl methacrylate implant: solutions of pitfalls.* A. El-Ghani, M. A. Wael. 2018, Egyptian Journal of Neurosurgery, Vol. 33, a.n. 7.

10. *Complications with PMMA compared with other materials used in cranioplasty: a systematic review and meta-analysis.* R. De Souza Leao, J. Raposo Souto Maior, C. Aparecido De Araújo Lemos, B. Cavalcanti Do Egito Vasconcelos, M. A. Japiassú Resende Montes, E. Piza Pellizer, S. L. D. Moraes. 2018, Brazilian Oral Research , Vol. 32, p. e31.

11. *Reconstruction of Cranial Vault Defect with Polyetheretherketone Implants.* P.Brandicourt, F. Delanoé, F. E. Roux, F. Jalbert, D. Brauge, F. Lauwers. 2017, World Neurosurgery, Vol. 105, p. 783 – 789.

12. *Comparative Cost-Effectiveness of Cranioplasty Implants.* A. Binhammer, J. Jakubowski, O. Antonyshyn, P. Binhammer. 2020, Plastic Surgery, Vol. 28, p. 29-39.

13. *Use of polyetheretherketone (PEEK) in orbital floor fracture reconstruction – A case for concern.* A. Jabar Nazimi, M. Md Yusoff, R.Nordin, S. Nabil. 2015, Journal of Oral and Maxillofacial Surgery, Medicine, and Pathology, Vol. 27, p. 536 – 539.

14. *Customized cost-effective polymethylmethacrylate cranioplasty: a cosmetic comparison with other low-cost methods of cranioplasty.* M. Baldia, M. Joseph, S. Sharma, D. Kumar, A. Retnam, S. Koshy, R. Karuppusami. 2022, Acta Neurochirurgica, Vol. 164, p. 655–667.

15. *Patient specific Polymethyl methacrylate customized cranioplasty using 3D printed silicone moulds: Technical note.* A. Scerrati, F. Travaglini, C. A. E. Gelmi, A. Lombardo, P. De Bonis, M. A. Cavallo, P. Zamboni. 2022, International Journal of Medical Robotics and Computer Assisted Surgery, Vol. 18, p. e2353.

16. *Customized and Cost – Effective 3D Printed Mold for Cranioplasty: India's First Single Center Experience.* S. Gopal, S. Rudrappa, A. Sekar, V. Preethish – Kumar, D. Masapu. 2021, Neurology India, Vol. 69, p. 611 – 617.

17. *Customized Polymethylmethacrylate Cranioplasty Implants Using 3 – Dimensional Printed Polylactic Acid Molds: Technical Note with 2 Illustrative Cases.* J. A. Hay, T. Smayra, R.d Moussa. 2017, World Neurosurgery, Vol. 105, p. 971 – 979.

18. *Surgical results of cranioplasty using three-dimensional printing technology.* Cheng-Hsin Cheng, Hao-Yu Chuang, Hung-Lin Lin, Chun-Lin Liu, Chun-Hsu Yao. 2018, Clinical Neurology and Neurosurgery, Vol. 168, p. 118-123.

19. *Cranioplasty with three-dimensional customised mould for polymethylmethacrylate implant: a series of 16 consecutive patients with cost-effectiveness consideration.* E. Barros Da Silva Júnior, A. H. De Aragão, M. De Paula Loureiro, C. Silva Lobo, A. F. Oliveti, R. Martinelli De Oliveira, R. Ramina. 4, 2021, 3D Printing in Medicine, Vol. 7, a.n. 4.

20. *3D-Printer-Assisted Patient-Specific Polymethyl Methacrylate Cranioplasty: A Case Series of 16 Consecutive Patients.* S. N. Schön, N. Skalicky, N. Sharma, D. W. Zumofen, F. M. Thieringer. 2021, World Neurosurgery, Vol. 148, p. e356-e362.

21. *Customized cranioplasty implants using three-dimensional printers and polymethyl-methacrylate casting.* B. J. Kim, K. S. Hong , K. J. Park , D. H. Park , Y.G. Chung , S. H. Kang. 2012, Journal of Korean Neurosurgical Society, Vol. 52, p. 541-546.

22. *Zauba* [Online] https://www.zauba.com/import-resomer-l-206-s-hs-code.html.

23. *A review of the manufacturing process and infection rate of 3D-printed models and guides sterilized by hydrogen peroxide plasma and utilized intra-operatively.* G. K.H. Shea, K. L. K. Wu, I. W. S. Li, M. F. Leung, A. L. P. Ko, L. Tse, S. S. Y. Pang, K.wan, K. Y. H. Kwan, T. M. Wong, F. K. L. Leung, C. X. Fang. 2020, 3D Printing in Medicine, Vol. 6, a.n. 7.

24. *Additively manufactured medical products – the FDA perspective.* M. Di Prima, J. Coburn, D. Hwang, J. Kelly, A. Khairuzzaman, L. Ricles. 2016, 3D Printing in Medicine, Vol. 2, a.n. 1.

25. *3DP World* [Online] https://3dpworld.it/prodotto/z-support-premium/?gclid=CjwKCAjwwo-WBhAMEiwAV4dybRhbS-905T2kWUG0NZaPZ7BDJiIQ4PAiO5zeYhFt0P-AiSx7xgksExoC1SAQAvD_BwE.

26. *talent* [Online] https://it.talent.com/salary?job=tecnico+informatico.

27. *servizi per utenze* [Online] https://serviziperutenze.it/pun-aggiornamento-dicembre-2020-prezzo-mercato-allingrosso/.

28. *westcmr* [Online] https://www.westcmr.com/43-1280-wb2-43-1280.

29. *Influence of different sterilization processes on the properties of commercial poly(lactic acid).* M. Savaris, V. Dos Santos, R. N. Brandalise. 2016, Materials Science and Engineering: C, Vol. 69, p. 661-667.

30. *Comparative study of different techniques for the sterilization of poly-L-lactide electrospun microfibers: effectiveness vs. material degradation.* A. Rainer, M. Centola, C. Spadaccio, G. Gherardi, J. A. Genovese, S. Licoccia, M. Trombetta. 2010, The International Journal of Artificial Organs, Vol. 33, p. 76-85.

31. *Are the common sterilization methods completely effective for our in-house 3D printed biomodels and surgical guides?* I. Aguado-Maestro, M. De Frutos-Serna, A. González-Nava, A. B. Merino-De Santos, M. García-Alonso. 2021, Injury, Vol. 52, p. 1341-1345.

32. *Evaluation of a Medical Grade Thermoplastic Polyurethane for the Manufacture of an Implantable Medical Device: The Impact of FDM 3D-Printing and Gamma Sterilization.* M. S. M'Bengue, T Mesnard, F. Chai, M. Maton, V. Gaucher, N. Tabary, M. J. García-Fernandez, J. Sobocinski, B. Martel, N. Blanchemain. 2023, Vol. 15, p. 456-469.

33. *CAD generated mold for preoperative implant fabrication in cranioplasty.* J. Wulf, L. C. Busch, T. Golz, U. Knopp, A. Giese, H. Ssenyonjo, S. Gottschalk, K. Kramer. 2005, Studies in Health Technology and Informatics, Vol. 111 , p. 608-610.

34. *Biocompatibility and biomechanical analysis of elastic TPU threads as new suture material.* R. R. Vogels, A. Lambertz, P. Schuster, S. Jockenhoevel, N. D. Bouvy, C. Disselhorst-Klug, U. P. Neumann, U. Klinge, C. D. Klink. 2017, Journal of Biomedical Materials Research. Part B: Applied Biomaterials, Vol. 105, p. 99-106.

35. *A Comprehensive Investigation on 3D Printing of Polyamide 11 and Thermoplastic Polyurethane via Multi Jet Fusion.* W. S. Tey, C. Cai, K. Zhou. 2021, Polymers, Vol. 13, p. 2139-2155.

36. *3D Printed Thermoelectric Polyurethane/Multiwalled Carbon Nanotube Nanocomposites: A Novel Approach towards the Fabrication of Flexible and Stretchable Organic Thermoelectrics.* L. Tzounis, M. Petousis, S. Grammatikos, N. Vidakis. 2020, Materials, Vol. 13, p. 2879-2894.

37. *Is toxicity of PMMA (paramethoxymethamphetamine) associated with cytochrome P450 pharmacogenetics?* M. Vevelstad, E. L. Øiestad, S. Bremer, I. L. Bogen, A. L. Zackrisson, M. Arnestad. 2016, Forensic Science International, Vol. 261, p. 137-147.

Table 1.

Nozzle diameter, mm	0.40
Layer thickness, mm	0.15
Print speed, mm/s	50
Extrusion Temperature, °C	210
Platform Temperature, °C	50
Infill Density, %	20
Fan, %	100
Type Infill	Cube
Raft	Enable
Support material	Z-SUPPORT Premium
Raft enabled	yes
Raft layers	5

Table 2.

Nozzle diameter, mm	0,40±0,01
Layer thickness, mm	0,15
Print speed, mm/s	30
Extrusion Temperature, °C	270
Platform Temperature, °C	90
Infill Density, %	10
Fan, %	Graduate from 0 to 40
Type Infill	Cube
Raft	Enable
Support material	TPU
Raft enabled	yes
Raft layers	5

Table 3.

Printing method / Step timing	Direct print	Two valves silicone mold	Two valves TPU mold
InVesalius 3.1	1 h Of which 40 min specialized computer technician	1 h Of which 40 min specialized computer technician	1 h Of which 40 min specialized computer technician
VxElements	3 h Of which 2h, specialized computer technician and radiology technician	3 h Of which 2h, specialized computer technician and radiology technician	3 h Of which 2h, specialized computer technician *and radiology technician*
Meshmixer	2 h (3 mm thickening) Of which, 10 min of specialized computer technician	3 h (5 mm thickening) Of which, in both cases, 10 min of specialized computer technician	2 h (3 mm thickening) Of which 10 min, specialized computer technician
SolidWorks	-------	-------	• Upper valve: 8 h; • Lower valve: 6 h All active projecting time (specialized computer technician)
Z-Suite	1 h Of which, 1h of specialized computer technician	---------	• Upper part: 15 min • Lower part: 15 min All active projecting time (specialized computer technician)
Simplify3D software	-------	1 h Of which, 1h of specialized computer technician	----
Total	7 h	8 h	20 h 30 min

Table 4.

STL file	7 h
Printing time	22 h 47 min
(+extra time of printing step)	30 min
Total	30 h 17 min

Table 5.

STL file	8 h
Printing time	9 h
(+extra time of printing step)	30 min
Hand manufacturing of two valve mold	1 h
Drying time of medical-grade silicone elastomer at R.T.	20 min
PMMA pouring	5 min
PMMA drying	10 min
Total	19 h, 5 min

Table 6.

STL file (total value, upper and lower valve)	20 h 30 min
Printing time	• Upper valve: 2 G 7 h 18 min • Lower valve: 1 G 18 h 32 min
(+extra time of printing step)	• Upper valve: 30 min • Lower valve: 30 min
PMMA pouring	5 min
PMMA drying	20 min
Total	119 h 45 min

Table 7.

	Direct print orthogonal	Direct print parallel	TPU mold orthogonal	TPU mold parallel	Silicone mold orthogonal	Silicone mold parallel
Thickness	3.30±0.04	3.16±0.01	3.3±0.1	3.18±0.06	2.85±0.1	2.9±0.2
Δ %	9.95	5.27	9.83	6.11	-5	3.3%
Width	13.1±0.4	12.9±0.01	12.5±0.1	12.5±0,2	12.51±0.1	12.6±0.2
SD %	3.26	1.84	-1.30	-1.81	-1.50	0.8 %
Length	128.0±0.3	126.8±0.2	125.50±0.5	124.3±0.9	127.95±	123.7±
SD %	0.76	-0.17	-1.19	-2.09	0.75	2.6 %

Table 8.

Sample	**(Ra ± s.d) µm**
Direct print - orthogonal	19.29±0.08
Direct print - parallel	18.7±0.1
TPU mold - orthogonal	37±2
TPU mold - parallel	42±2
Silicone mold - orthogonal	2.23±0.09
Silicone mold - parallel	2.9±0.1

Table 9.

Scenario	**Flexural Modulus, MPa**
Direct print - parallel	2974 ± 5
Direct print - orthogonal	2300 ± 200
TPU mold - parallel	2200 ± 100
TPU mold - orthogonal	1400 ± 200
Silicone - mold parallel	1700 ± 200
Silicone - mold orthogonal	1700 ± 200

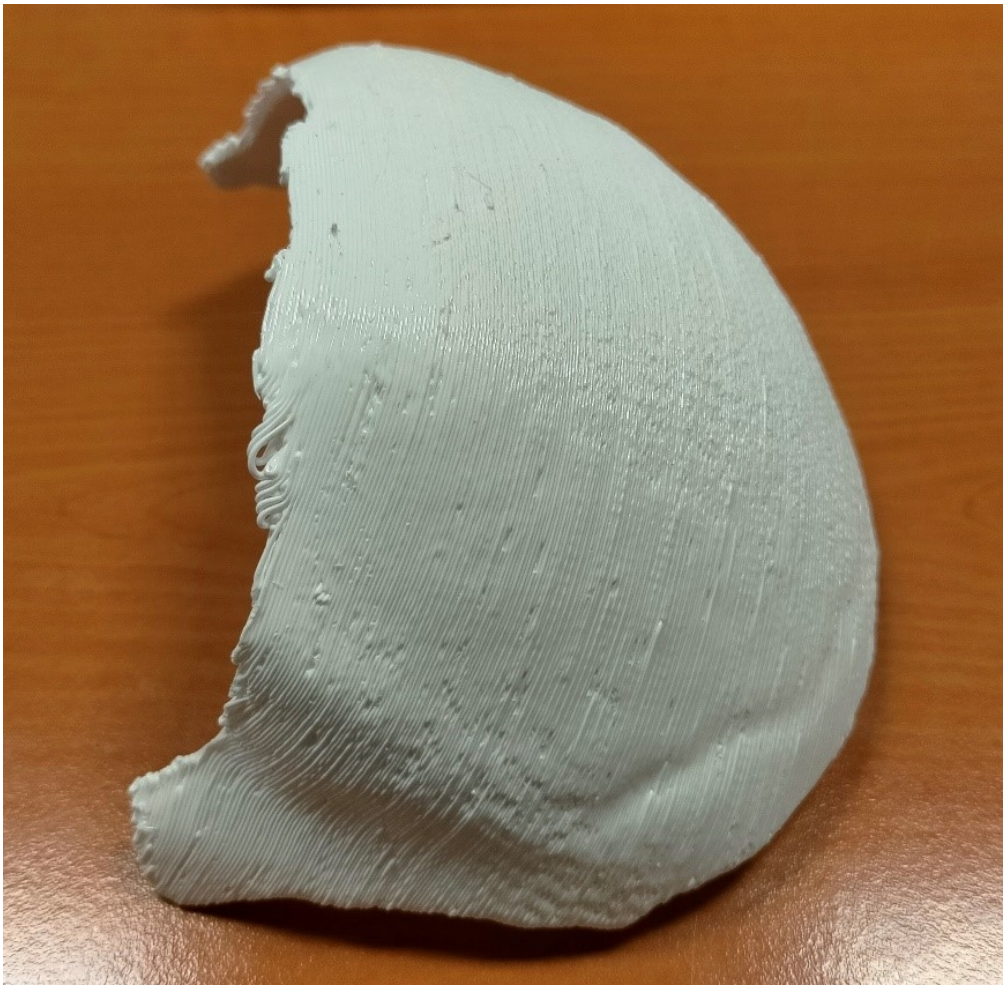

Figure 1 3D-printed master in ABS of the cranial flap.

99x98mm (220 x 220 DPI)

Figure 2 Schematic representation of the silicon mold during the phase of cranial flap extraction

131x128mm (144 x 144 DPI)

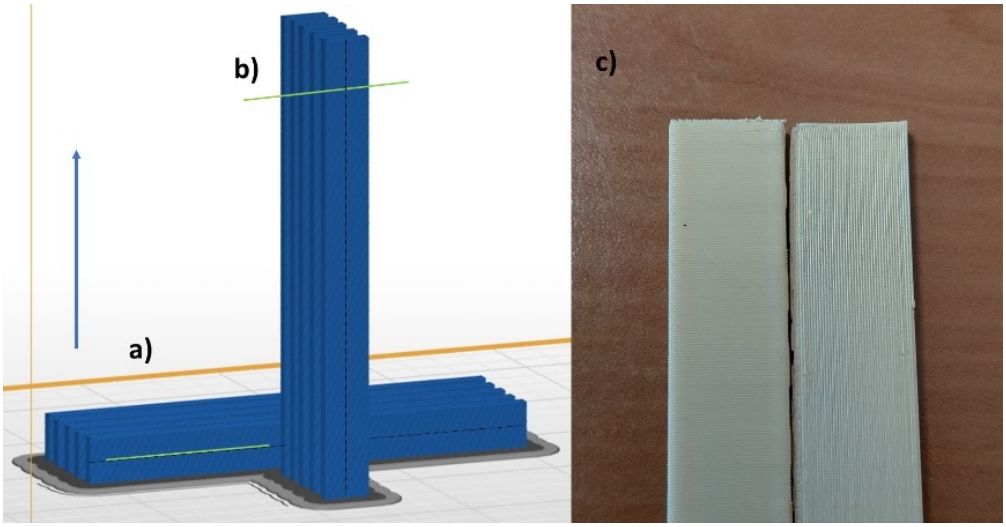

Figure 3 "Direct print"scenario: STL files file of a) parallel and b) orthogonal samples; c) printed samples in the two orientations

99x51mm (220 x 220 DPI)

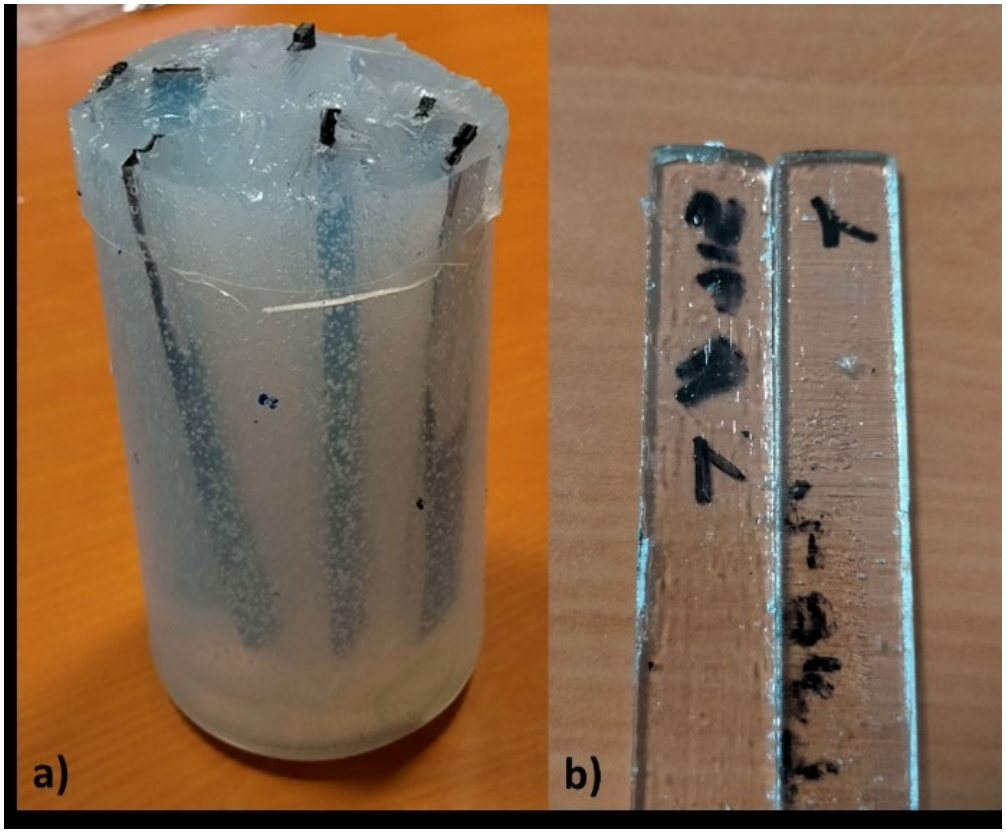

Figure 4 "silicone mold" scanario: a) preparation of silicone mold with ABS masters; b) cast samples in the two orientations.

80x66mm (220 x 220 DPI)

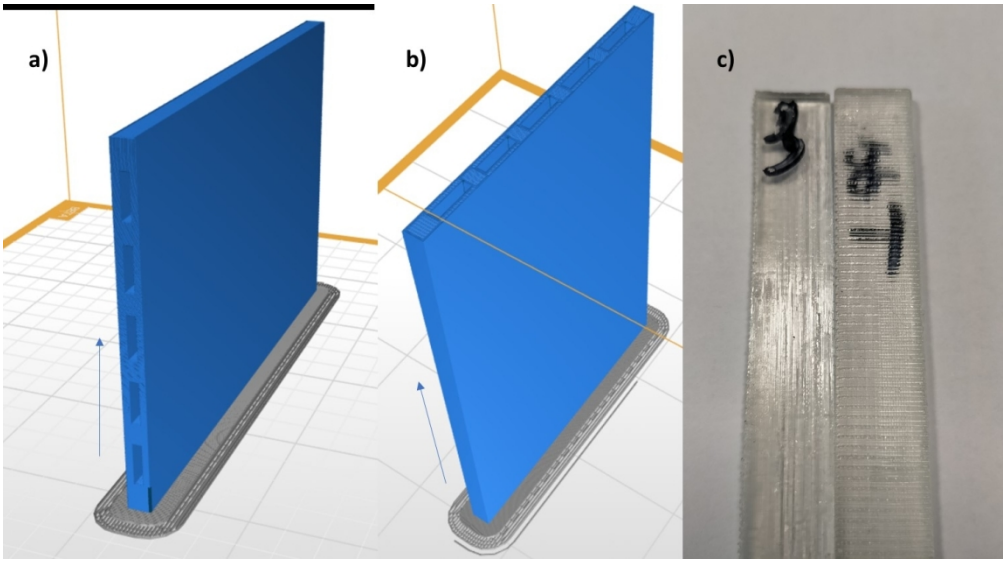

Figure 5 "TPU mold" scenario: STL file of a) parallel mold and b) orthogonal mold; c) cast samples in the two orientations

254x141mm (150 x 150 DPI)

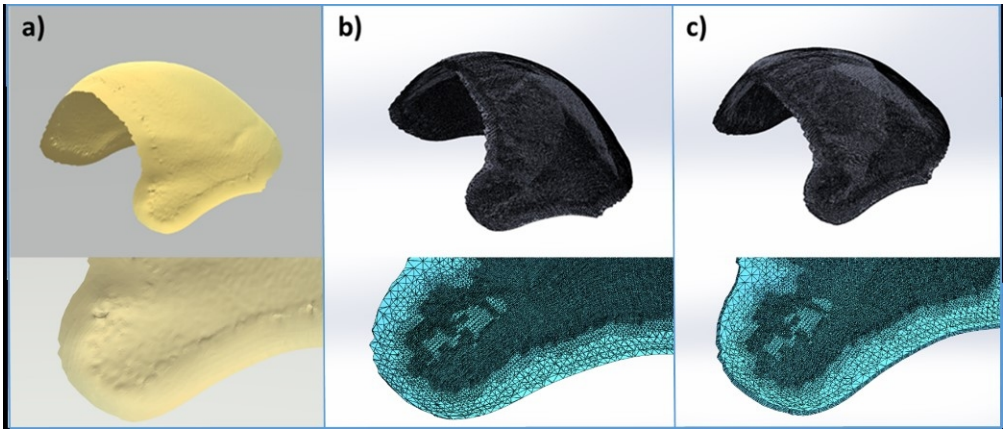

Figure 6: Images of a selected section of patient's cranium, selected as model for the implant manufacturing: a) 3D model of cranium surface; b) same surface after meshing process; c) model after thickening and the second step of meshing.

120x51mm (220 x 220 DPI)

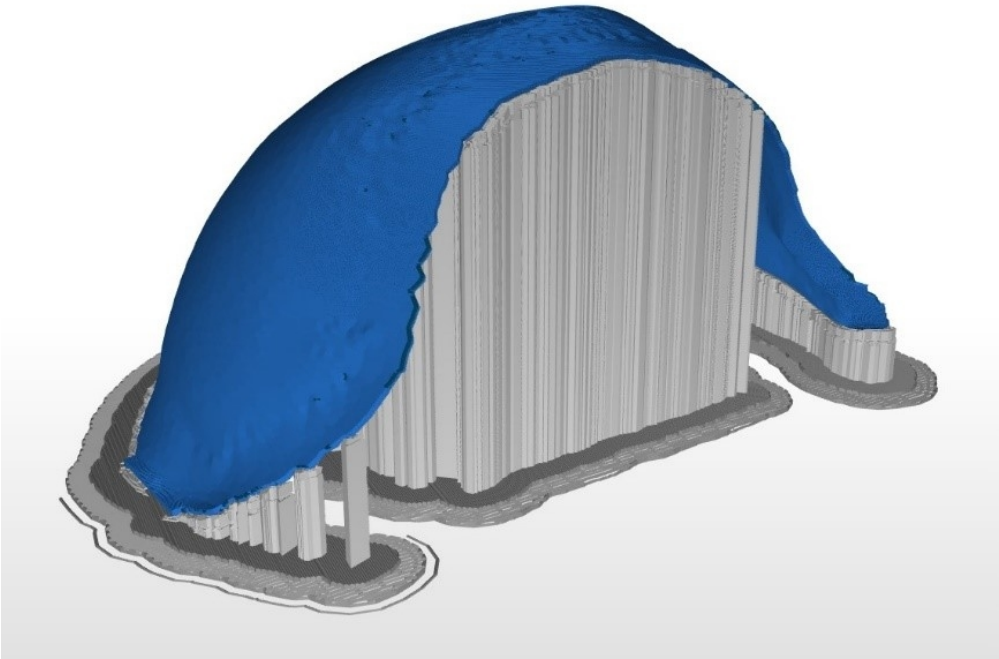

Figure 7 Slicing file of 3 mm PLA skull cap.

99x69mm (220 x 220 DPI)

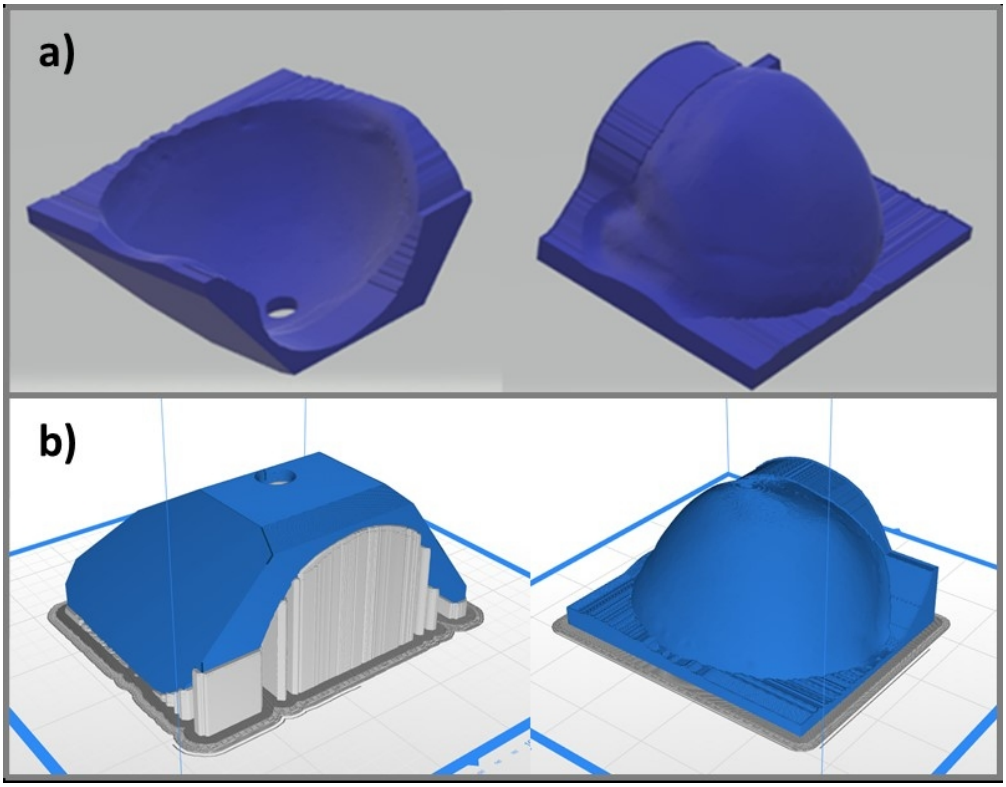

Figure 8 3D image of a) upper mold half (left) in upside down position, and lower mold half (right) in upside down position; b) slicing files of structures as in a)

136x106mm (150 x 150 DPI)

Figure 9 Cranial flap obtained from direct printing of PLA filament

125x114mm (96 x 96 DPI)

Figure 10 PMMA cranial flap obtained from silicone mold (15)

90x49mm (220 x 220 DPI)

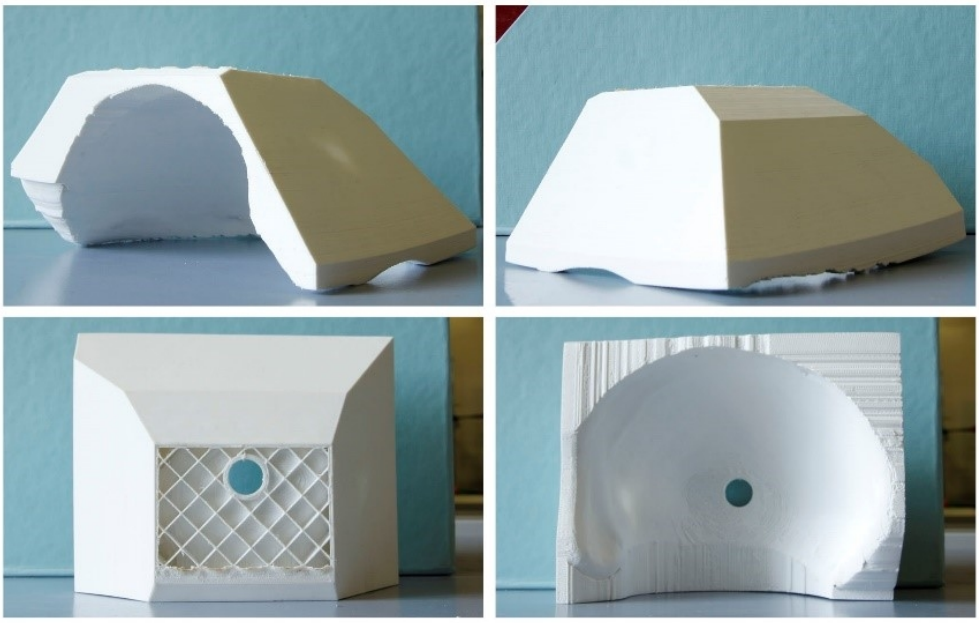

Figure 11 Views of upper mold half of printed TPU mold.

99x64mm (220 x 220 DPI)

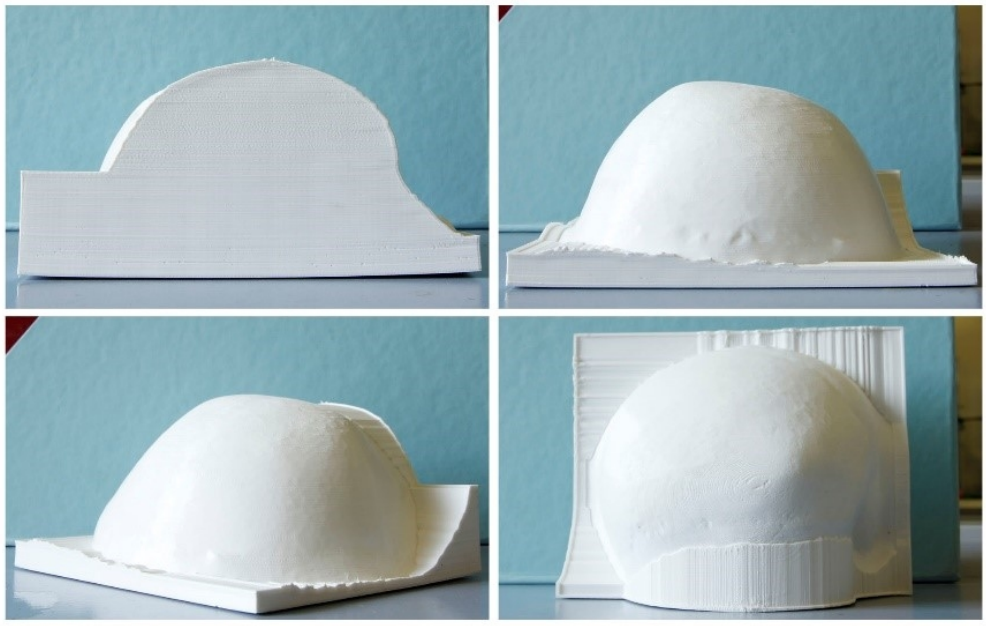

Figure 12 Views of lower mold half of printed TPU mold.

99x64mm (220 x 220 DPI)

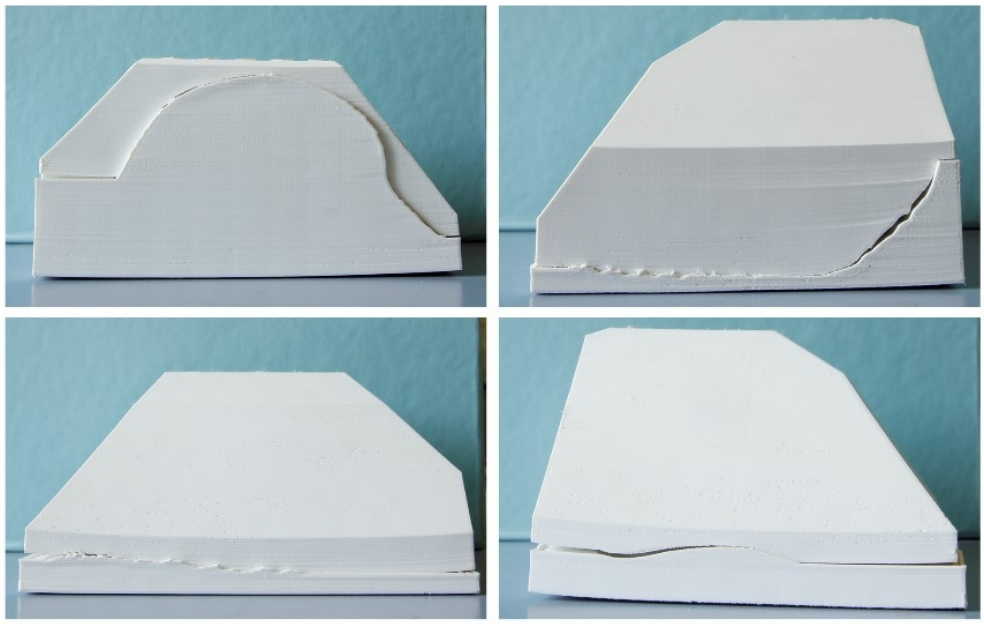

Figure 13 Views of two valves mold of printed TPU mold.

99x64mm (220 x 220 DPI)

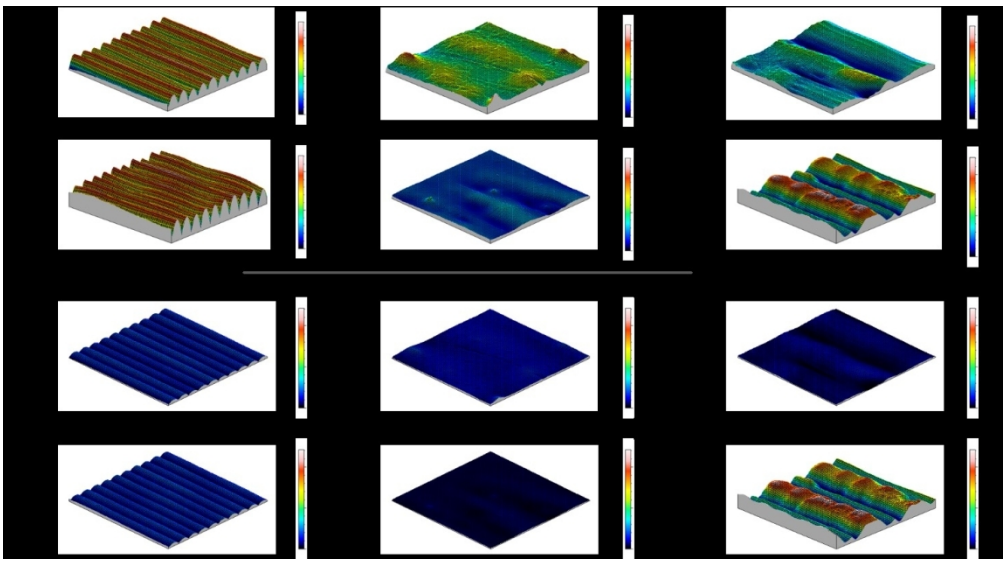

Figure 14 Morphological maps under adapted scale (from a) to f) plots) and normalized scale (from a') to f') plots) of slab samples obtaine by: a), a') parallel and b), b') orthogonal PLA direct print; c), c') parallel and d), d') orthogonal silicone mold; e, e') parallel, f), f') orthogonal TPU mold.

170x94mm (220 x 220 DPI)

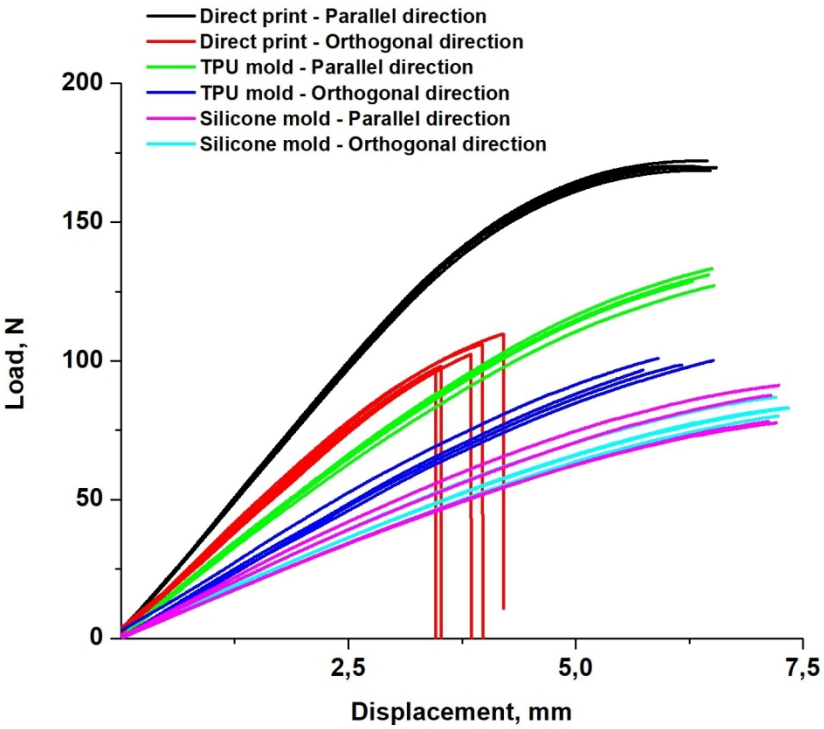

Figure 15 Load-displacement curves for flexural tests

349x269mm (120 x 120 DPI)